Brigham Young University
BYU ScholarsArchive

All Theses and Dissertations

2009-04-17

A Numerical Model of the Friction Stir Plunge

Stanford Wayne McBride
Brigham Young University - Provo

Follow this and additional works at: https://scholarsarchive.byu.edu/etd

 Part of the Mechanical Engineering Commons

BYU ScholarsArchive Citation

McBride, Stanford Wayne, "A Numerical Model of the Friction Stir Plunge" (2009). *All Theses and Dissertations*. 1772.
https://scholarsarchive.byu.edu/etd/1772

This Thesis is brought to you for free and open access by BYU ScholarsArchive. It has been accepted for inclusion in All Theses and Dissertations by an authorized administrator of BYU ScholarsArchive. For more information, please contact scholarsarchive@byu.edu, ellen_amatangelo@byu.edu.

A NUMERICAL MODEL OF THE FRICTION STIR PLUNGE

by

Stanford W. McBride

A thesis submitted to the faculty of

Brigham Young University

in partial fulfillment of the requirements for the degree of

Master of Science

Department of Mechanical Engineering

Brigham Young University

August 2009

Copyright © 2009 Stanford W. McBride

All Rights Reserved

BRIGHAM YOUNG UNIVERSITY

GRADUATE COMMITTEE APPROVAL

of a thesis submitted by

Stanford W. McBride

This thesis has been read by each member of the following graduate committee and by majority vote has been found to be satisfactory.

Date	Carl D. Sorensen, Chair
Date	Tracy W. Nelson
Date	Michael P. Miles

BRIGHAM YOUNG UNIVERSITY

As chair of the candidate's graduate committee, I have read the thesis of Stanford W. McBride in its final form and have found that (1) its format, citations, and bibliographical style are consistent and acceptable and fulfill university and department style requirements; (2) its illustrative materials including figures, tables, and charts are in place; and (3) the final manuscript is satisfactory to the graduate committee and is ready for submission to the university library.

Date

Carl D. Sorensen
Chair, Graduate Committee

Accepted for the Department

Larry L. Howell
Graduate Coordinator

Accepted for the College

Alan R. Parkinson
Dean, Ira A. Fulton College of Engineering and Technology

ABSTRACT

A NUMERICAL MODEL OF THE FRICTION STIR PLUNGE

Stanford W. McBride

Department of Mechanical Engineering

Master of Science

A Lagrangian finite-element model of the plunge phase of the friction stir welding process was developed to better understand the plunge. The effects of both modeling and experimental parameters were explored,

Experimental friction stir plunges were made in AA 7075-T6 at a plunge rate of 0.724 mm/s with spindle speeds ranging from 400 to 800 rpm. Comparable plunges were modeled in Forge2005. Various simulation parameters were explored to assess the effect on temperature prediction. These included the heat transfer coefficient between the tool and workpiece (from 0 to 2000 W/m-K), mesh size (node counts from 1,200 to 8,000), and material model (five different constitutive relationships). Simulated and measured workpiece temperatures were compared to evaluate model quality.

As spindle speed increases, there is a statistically significant increase in measured temperature. However, over the range of spindle speeds studied, this difference is only

about 10% of the measured temperature increase. Both the model and the simulation show a similar influence of spindle speed on temperature. The tool-workpiece heat transfer coefficient has a minor influence (<25% temperature change) on simulated peak temperature. Mesh size has a moderate influence (<40% temperature change) on simulated peak temperature, but a mesh size of 3000 nodes is sufficient. The material model has a high influence (>60% temperature change) on simulated peak temperature. Overall, the simulated temperature rise error was reduced from 300% to 50%. It is believed that this can be best improved in the future by developing improved material models.

ACKNOWLEDGMENTS

I am extraordinarily grateful to all who have helped me to accomplish this work and gain a great education at this blessed institution. I would like to thank specifically: Dr. Carl Sorensen, for teaching me how to think and how to work; Dr. Mike Miles, for sharing with me the excitement of the program and project; Dr. Tracy Nelson, for providing this opportunity. Especially I would like to thank my family for the years of support and my eternal bride, Jenny McBride, for providing me the motivation to finish.

TABLE OF CONTENTS

LIST OF TABLES

LIST OF FIGURES

1. Introduction

1.1. Friction Stir Welding

Friction stir welding is a solid state joining process producing material properties generally superior to traditional forms of welding. Friction stir technology was pioneered at The Welding Institute of the UK in 1991 (Thomas, 1991). The basic premise of the process is that a distinctly designed, rotating tool is plunged into the workpiece material or between two materials the operator desires to join. In a butt weld the rotating tool then traverses along the seam between the two materials and thermo-mechanically joins the two pieces as seen in Figure 1.

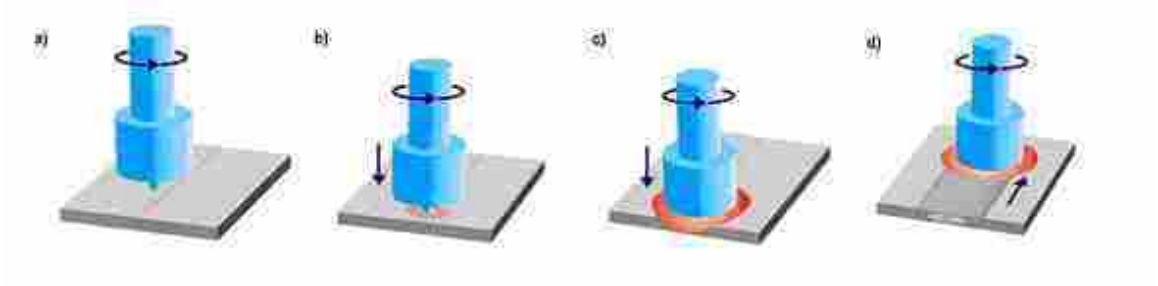

Figure 1 - Illustration of the friction stir process, (a) rotation of the tool, (b) plunge of the tool, (c) completion of the plunge, (d) traverse. (Oliphant, 2004)

1.2. Numerical Modeling

Numerical modeling is one of the best ways to understand a complex process, such as friction stir welding. The basic premise of numerical modeling is that a medium is subdivided into discrete or finite elements. A computer simulation then models the behavior and properties of each of these elements as they are acted upon by an external force by multiple sets of governing laws and physical equations. Due to computational limitations, simplifying assumptions are made to reduce complexity and computational processing time. As friction stir welding is not well understood, it is a candidate for numerical modeling.

Numerical applications used for better understanding the friction stir process vary from single solution multivariate equations to time dependent graphical models. Two-dimensional models have been used to approximate the heat distribution through the workpiece, but typically focus on the traverse portion of the process. Three-dimensional models give insight into the depth component of the process. These models usually focus on simplified heat inputs or used a fluid flow method that also concentrates on the traverse portion of the process.

Because the friction stir weld plunge is a transient, three-dimensional process a more complex modeling program is required. Work done by Oliphant (2004) determined that Forge3, a modeling program produced by Transvalor of France, showed potential in accurately modeling the plunge. The program has subsequently been updated and is known as Forge2005. This software package is allows for a fully defined three-dimensional workpiece, a rotating tool interface, a variety of material laws, and parameter selection. Oliphant was able to show the friction stir plunge could be modeled, but did not explore the capabilities of the program or the various effects of changing the parameters within the simulation. A later study by Lasley (2005) showed that modification of specific parameters within the simulation could improve the accuracy of the model and these parameters could be defined by comparison to experimental testing.

Numerical models, especially Forge2005, typically contain multiple options for the user to change and control. This flexibility is advantageous as it allows the user to created models that more accurately represent the true process. But this flexibility is also challenging as the large number of adjustable parameters can overwhelm the user. The interactions of multiple changes can obscure the influence of any single parameter on the resulting simulation.

1.3. Thesis Statement

The friction stir plunge is a transient process that is better understood through numerical modeling and experimental testing. This work intends to improve the modeling of the friction stir plunge. Better friction stir plunges and numerical models are created when the associated parameters influencing the behavior are understood. The understanding of the effects of selected parameters is achieved through the study of simulations conducted in Forge2005, a series of related experimental results, and the comparison of simulation and experiment.

The areas of study that are given specific consideration in experimentation are the influence of spindle speed and the behavior during the plunge and during the dwell. The focus of the parameter study is the influence and significance of the heat transfer coefficient between the tool and the workpiece, the influence of mesh size, the capability of material model, and the influence of spindle speed on the temperature in the workpiece. Each of these areas of study defines the behavior or significance of a parameter that influences the temperatures observed in the friction stir plunge process.

2. Background

Friction stir processing has captured the interest of groups the world over as the process becomes more reliable, the safety in performing the weld is known, and the quality of the weld is recognized. Academics and industry alike have studied portions of the friction stir process and additional modifications of and applications for the process are discovered each year. Computer models are used by researchers to understand the friction stir process and learn about the laws that govern the process. Simulation and experimental research have laid a rich foundation for numerical modeling research and comparative experimentation.

2.1. Numerical Modeling

Numerical modeling is a continually expanding field of research and technological improvement. Basic numerical modeling simplifies engineering processes by reducing an infinitely fine medium into discreet portions, applying a fixed set of mechanical, material, and other laws to modify the medium, and produce usable results. Through advances in hardware and software greater detail in simulation have produced better results in a shorter time frame.

The software used to numerically model a process must cope with the complexities of the process. The friction stir process is very complex and presents a challenge to traditional modeling programs. Oliphant (2004) noted some of the complex characteristics included:

- A wide range of stress, strain, and strain rate
- A wide range of temperatures (room temperature to near melt temperature)
- Plastic deformation within the workpiece
- Frictional heating and plastic deformation heating
- A wide range of pressure zones
- Rotational tooling
- Heat transfer between the tool, the anvil, the ambient medium and throughout the workpiece.

2.2. Forge2005

Forge2005 is a numerical modeling program that has emerged as a capable program in friction stir modeling. Forge2005 is a complex, closed-source finite-element computational package produced by Transvalor SA of France (Transvalor, 2005). The software package offers the advantage of a self-contained pre-process viewer, the computational processor, and a post process viewer. The program's primary purpose is to facilitate numerical models of traditional forging processes. However, the robust and comprehensive nature of the models allows the tool to be used for the modeling of the friction stir plunge.

This program has gained acceptance in industry from several capabilities of the program. The material definition libraries are extensive and contain good material properties in the regions of traditional forging and forming operations (Transvalor, 2005). The code uses Lagrangian finite elements with frequent remeshing to accommodate for material movement. Functions are

multivariate functions with the primary parameters of strain, strain rate, and temperature to determine the flow stress in each cell through a simulation. These characteristics give Forge2005 the ability to handle a high temperature, high deformation process.

2.3. Friction Stir Process Prior Work

The majority of the research into the process has focused on the traverse portion of the weld process as this is the most predominant portion of the welding process. This steady state allows researchers to focus on single solution answers instead of a dynamic solution that varies in time. Research tends to center on the unique flow patterns that occur within the weld and heating of the material or workpiece. Both of these emphases help researchers to know of the unique behavior of friction stir processing and the material properties resulting from processing. However, the single solution result from the study of the traverse process offers little information about the transient behavior observed during the plunge.

Multiple codes exist today as tools for finite element modeling. Two-dimensional models have been used to explore the friction stir process. These works concentrate on the traverse portion of the weld and consider modeling from either a heat input perspective or a viscous fluid flow perspective. Dong et al. (2000) explored the base behaviors of the friction stir process and observed material heating in the stir zone. Song et al. (2003) uses a Lagrangian solution method to solve for the temperature and other properties in the workpiece through the course of a traverse. Numerical results show a symmetric heating pattern around the tool as the traverse process proceeds as seen in Figure 2. Chen et al. (2003) demonstrates a comparison between experimental temperatures and numerical solution temperatures. Shi et al. (2003) showed there was value in material models that varied the stress as a function of temperature and strain. Chao et al. (2003) developed specific results around the heat transferred between the workpiece and

other areas of the process. Each study seeks to define parameter interaction with the numerical model and the comparison to experimental behavior.

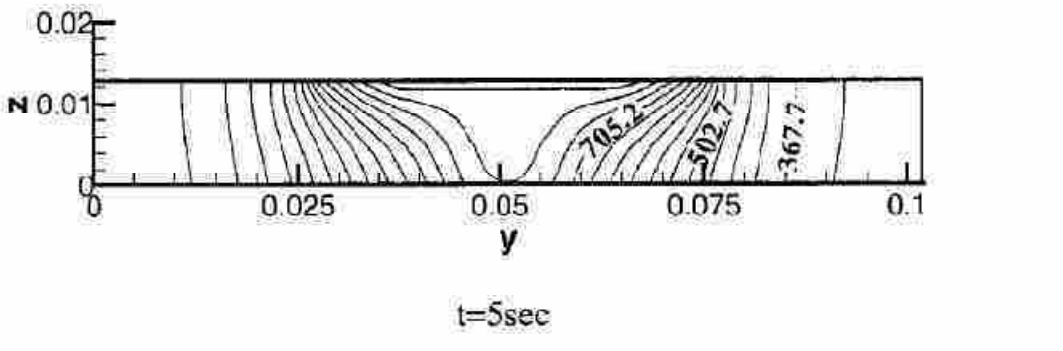

Figure 2 - Song (2003) demonstrates in steel the heating pattern observed found in the y-axis of a friction stir traverse.

Three-dimensional modeling has added to the understanding that behavior changes with depth. Bendzsak et al (2000), Colegrove et al (2000) and Ulysee (2002) used a fluid material model with high viscosity. Bendzsak et al. (2000) used the comparison of the post-welded traverse cross section in comparison with the single state solutions of the material flow and tracer flow. Colegrove et al. (2000) developed a series of vector equations that model the material behavior immediately around the tool. Figure 3 shows how this study used a comparison of simulation temperature and experimental temperature at specific locations in the workpiece to evaluate the model. Ulysee (2002) developed numerical models that compared the thermal behavior of around the tool as a function of spindle speed and validated temperature with experimentation. All of these experiments considered results at varied depths and validated the numerical models with experimentation.

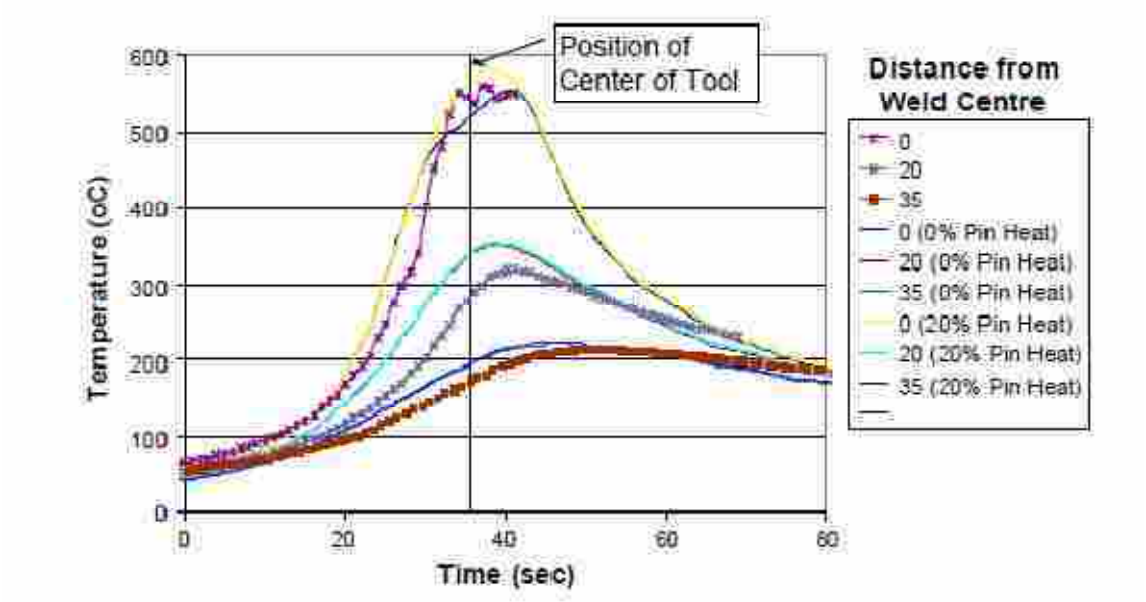

Figure 3 - Colegrove (2000) compared experimental and simulation temperature data 3 mm below the surface to validate a numerical model.

These prior works do not address the individual influence of each of the parameters: heat transfer coefficient, material model, mesh size, and spindle speed. These works also do not specifically address the plunge and the heating and temperature behaviors that occurring during the plunge. This work intends to define the influence of these parameters in isolation and demonstrate the temperature behaviors during the plunge.

2.4. Friction Stir Plunge Prior Work

The work completed in this study benefits greatly from work completed by Alma Oliphant (Oliphant, 2004). One of the basic objectives of Oliphant's work was to show if Forge2005 could be used for modeling. Oliphant developed the basic methods and tools that are

used for modeling in this research. This work expands the research done by Oliphant and specifically quantifies the behavior of certain parameters found within Forge2005.

Oliphant's work also compared simulation data to experimental data. Figure 4 and Figure 5 represent the results of the simulation and the experiment respectively. This study was limited in several ways. The plunge was limited to 6 seconds and did not give sufficient time for the a region where only the pin plunge behavior could be observed before the shoulder contacted the workpiece. Oliphant also used only adiabatic heat transfer, a single mesh size, only the hot material model, and a single spindle speed. The thermocouples and sensors only occurred at one depth preventing comparison of the impact of the thickness on the result. However, Oliphant produced a basic simulation that yielded verifiable results.

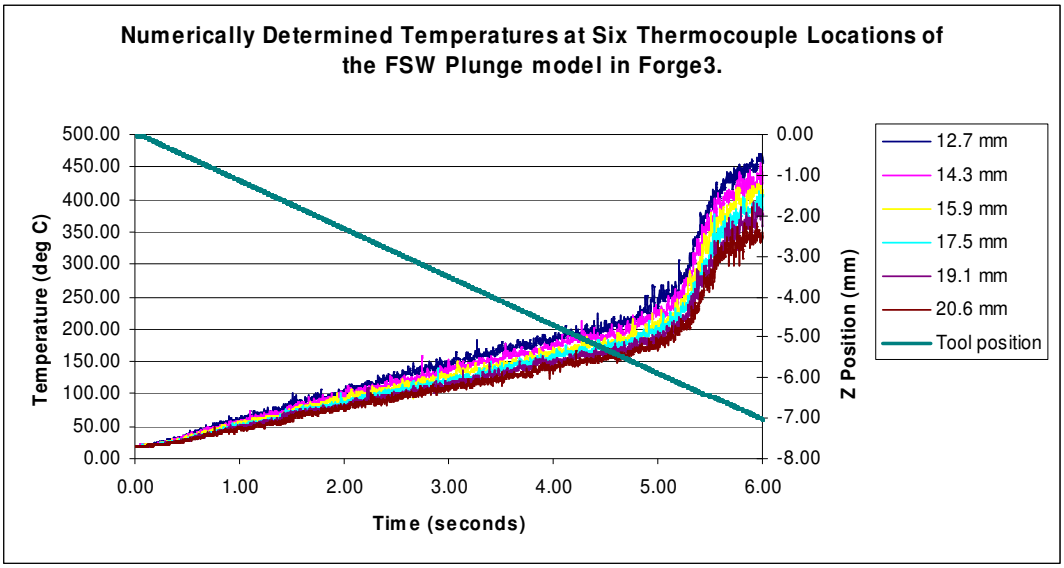

Figure 4 - Numerical simulation thermocouple data from Oliphant (2004) work.

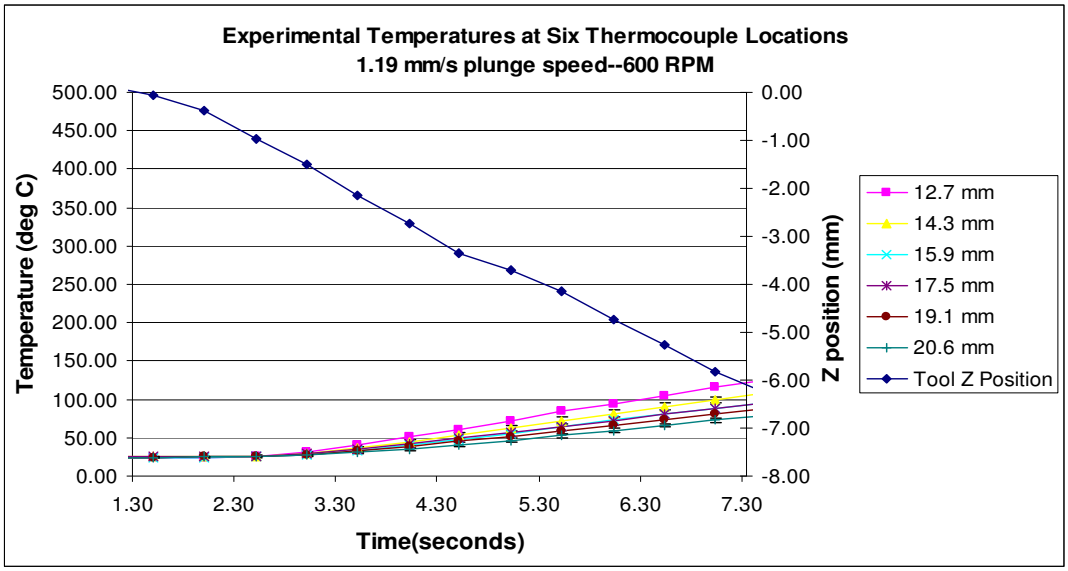

Figure 5 - Experimental simulation thermocouple data from Oliphant (2004) work over 6 seconds.

A seen from the figures above the comparison between the experimental temperatures and simulation temperatures is very different. Experimental temperatures barely reach 125°C by the end of the plunge phase while simulation temperatures reach above 450°C. This work intends to improve the friction stir model by reconciling the experimental temperatures and simulation temperatures. This is to be accomplished by closely defining the influence of selected parameters in the simulation.

2.5. Conclusion

A comparative study of numerical models with experimental results will provide better understanding of the friction stir plunge and the influencing parameters. Forge2005 has been shown to be a program capable of modeling the friction stir plunge. Prior work by other researchers has shown the interaction of multiple parameters can change the result. No study

defines the individual effects of specific parameters. This work intends to demonstrate the influence of the heat transfer coefficient between the tool and the workpiece, mesh size, material model, and spindle speed on the temperature in the workpiece; the significance of the heat transfer coefficient; and the behavior during the dwell and during the plunge as compared to the simulation temperatures.

3. Methodology

An experimental test series and an array of numerical models are used to understand the influence and significance of specific parameters and the temperature curve shape of the plunge process. Ten experimental tests were performed to determine the behavior of the workpiece at five different spindle speeds. A series of seventeen simulations are used to test the parameters of the spindle speed, mesh size, material model, and heat transfer coefficient between the tool and workpiece. Both the experiments and the simulations had thermocouples or sensors in the workpiece at comparable locations to record the workpiece temperatures during the course of the plunge. These temperature measurements provide the method for evaluation within the experimental series and simulations array or between the experimental and simulation.

3.1. Plunge Experiments

3.1.1. Equipment

Experimental tests were performed on Brigham Young University's RM2 gantry style friction stir welding machine from TTI. The RM2 is designed with a native computer controlled interface to control feeds and speeds and record thermocouple data channels. The RM2 used can be seen in Figure 6.

Figure 6 - Photograph of RM2 gantry style friction stir welding machine.

3.1.2.Data Acquisition

Two data acquisition processes were used for the collection of data from the experimentation. Native to the friction stir welding machine was a data acquisition device that device sampled at a rate of 9-10 times per second. The friction stir machine used low power radio waves to transmit a signal from the K-type thermocouple to a stationary antenna. Eight K-type thermocouples also connected to the control computer. The eight channels used were the outer-most eight holes of the eleven drilled for sampling.

Three other K-type thermocouples were used that sampled 500-600 times per second. Knowing from the exploratory experimentation that the area closest to the pin experienced the most dynamic change these faster thermocouples were used in the three holes closest to the pin. A program for collecting the data was written by Daryl Stratton of the BYU Friction Stir Research

Laboratory. This program was installed on a local laptop and connected to the machine control computer for the friction stir machine.

3.1.3. Thermocouples

Workpiece samples were prepared from Al 7075-T6 material 5/16 inches thick. Each piece was edge milled and cleaned for consistency. Sensor holes were drilled to match a radial pattern around the center of the workpiece in alignment with the tool center. All holes had an unimpeded path to the center of the heat source. A diagram of the resulting radial array is seen in Figure 7. The sample workpieces were 203.2 mm by 203.2 mm. Using the lower left corner as the origin, position and depth are listed in Table 1.

Table 1 - Physical position of thermocouple holes in test plate where (0,0) is the center of the plate.

Thermocouple	r (mm)	θ (deg)	Depth (mm)
TC1	0	0.	0.5
TC2	5	0.	3
TC3	6	205.	6.5
TC4	12	108.	6.5
TC5	15	294.	6.5
TC6	21	227.	6.5
TC7	27	29.	6.5
TC8	9	343.	3
TC9	12	71.	3
TC10	15	245.	3
TC11	21	312.	3
TC12	27	150.	3

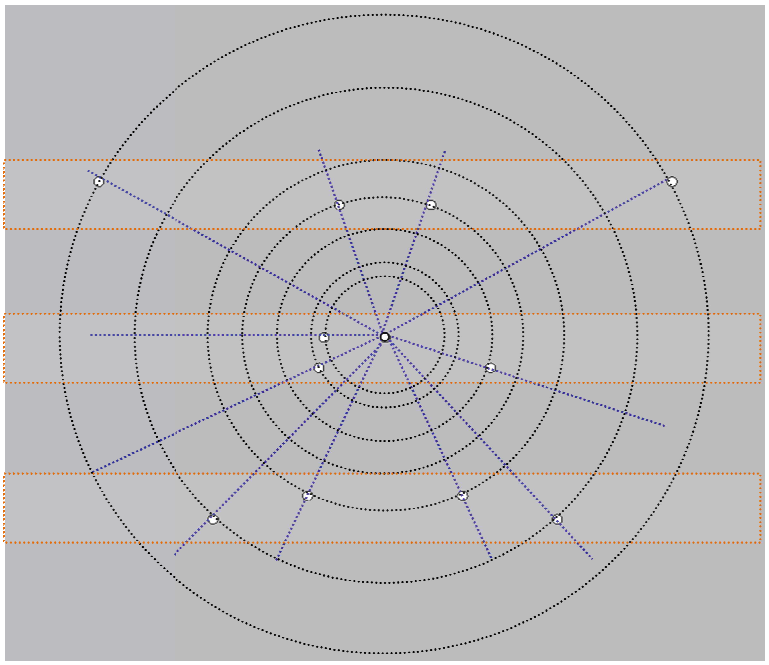

Figure 7 - Diagram of radial array of sensor holes in workpiece samples. The orange boxes represent the access channel locations.

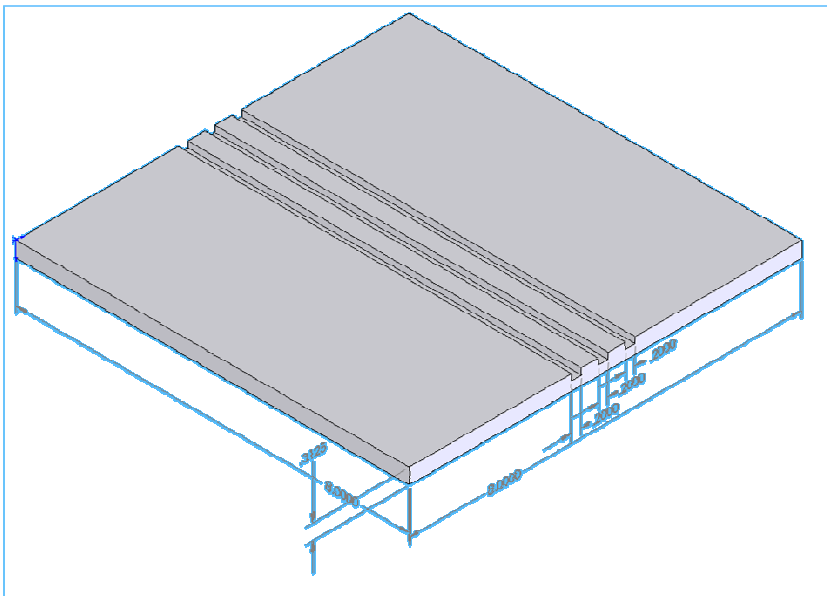

Figure 8 – CAD projection of secondary anvil allowing thermocouple probes to exit back of workpiece. All distance is in inches.

Sensors were fit into each sensor hole and a channeled backing plate was clamped to each workpiece sample prior to the plunge. This backing plate allows the thermocouples an exit channel and the ability to collect data during the plunge without being crushed. This plate is seen in Figure 8 and Appendix A. The workpiece and backing plate were clamped to a fixture on the RM2.

3.1.4. Plunge Sequence

The plunge duration is set at ten seconds to facilitate the observation of pin behavior and shoulder behavior. The plunge sequence was as follows. The tool was positioned 12.7 mm from the surface of the plate. The tool plunged 12.57 mm at a constant spindle speed of 500 rpm. The spindle speed was then adjusted to the desired value while the tool plunged to the depth of 7.24 mm. From the point of contact with the surface of the workpiece to the end of the plunge was 10 seconds in length. The tool dwelled at the end of the plunge for 5 seconds and was then extracted from the workpiece. Each plunge followed the same sequence and varied only in spindle speed.

3.1.5. Test Sequence

Five spindle speeds were tested. These speeds are 400, 500, 600, 700, and 800 rpm. Experimental plunges were conducted twice at each speed yielding ten total plunges. Plunges were run in a random pattern; the sequence is listed in Table 2.

Table 2- Experimental run sequence.

Run Sequence
400-1
800-1
700-1
400-2
500-1
600-1
700-2
500-2
600-2
800-2

3.2. Forge2005 Simulations

All work was performed in Forge2005 – Service Pack 1, running on a computer with Windows XP Professional with Service Pack 2, two Intel Pentium D processors 3.40 GHz, 2.0 GB cache, 2.00 GB of RAM. All computational times are based on performance from this computer.

Non-tested parameters are established through prior experimentation and work done by Lasley (2005). Base parameters were a ten second plunge at a 600 rpm spindle speed. Heat transfer coefficients were strong between the tool and the workpiece, ambient between the workpiece and the environment, and strong between the workpiece and the anvil. Material was Aluminum 7075 for the workpiece and mild steel for the tool with a mild steel surface condition representing the anvil. Mesh size was medium, as explained is a later section, by default. Material model was the hot rheology by default. Tool configuration was a smooth pin tool, pin depth of 7.20 mm, shoulder depth of 6.35 mm, pin radius of 3.18, tool radius of 12.7 mm. Workpiece configuration was a square plate 203.2 mm by 203.2 mm 7.9375 mm thick. The anvil was a

surface condition 220 mm by 220 mm by 0 mm. The native material model used a Norton-Hoff approximation method and a constant thermal conductivity in the workpiece.

3.2.1.Simulation

Seventeen variation simulations are reported in this study. Five simulations are used to test spindle speed at 400, 500, 600, 700, and 800 rpm. Three simulations are used to test mesh size and are called small, medium and large mesh size simulations. Five simulations are used to study the impact of material model on the simulations. These simulations are called hot rheology, cold rheology, rh7, rh9, and rh10 in reference to the material model used. Hot rheology and cold rheology refer to system defined models and rh7, rh9, and rh10 material models refer to user defined models. Four simulations are used to test for thermal exchange and are called adiabatic, weak, medium, and strong in reference to the heat transfer coefficient between the tool and workpiece. When the parameter is not being tested the mesh size is medium, the material model is hot rheology, and strong heat transfer between the tool and workpiece.

3.2.2.Tool Temperature

The tool has a specified time-dependent temperature that provides a boundary condition for the workpiece. Figure 9 shows a plot of the tool temperature as input into Forge2005. Data for the input used is seen in Table 3.

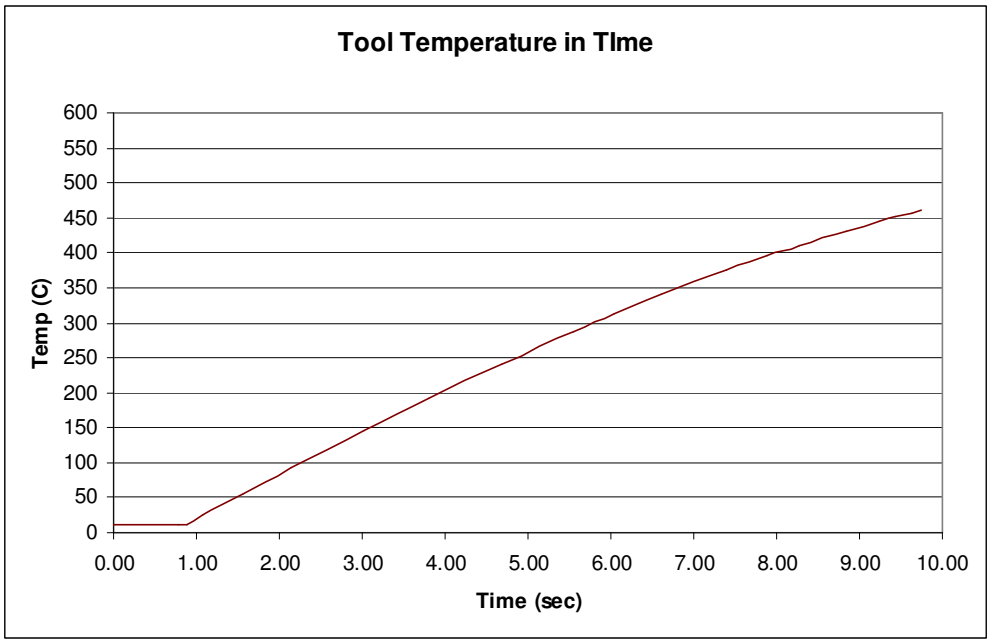

Figure 9 - Plot of input tool temperature in all simulations.

Table 3 - Time and temperature values for tool in simulation.

Simulation Time	Simulation Temperature
0.00	11.0
0.78	11.0
0.88	12.5
1.08	24.6
1.56	55.2
2.15	91.6
3.02	145.2
3.81	192.0
4.68	241.6
5.55	288.1
6.04	312.8
6.62	340.4
7.39	375.0
7.88	395.0
8.27	410.2
8.85	431.1
9.23	444.1
9.43	450.6
9.63	456.6

3.2.3.Sensors

Sensor placement is critical to the objective of comparable studies between simulation and experimental testing. Twelve thermocouples or sensor locations are used in both the simulations and the experiments. A list of the exact positioning for the sensors is found in Table 4. Two depths are used to allow for top to bottom comparison. These depths are 3 mm from the base of the plate and 6.5 mm from the base. The plate is 7.94 mm thick. The radial distance is selected to be as close as possible to the tool and then grouped 3 mm apart near the shoulder and 6 mm apart furthest from the tool.

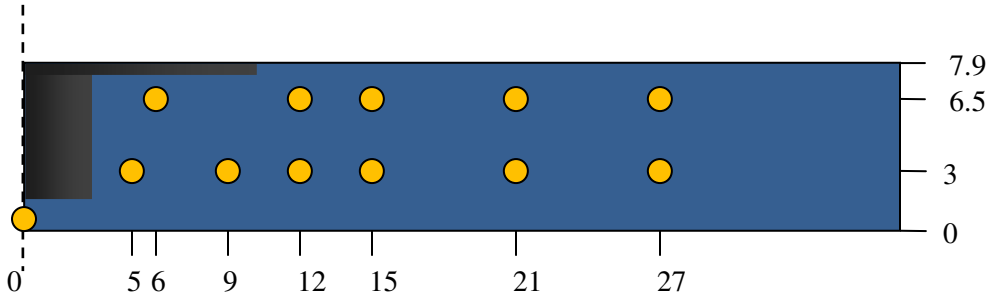

Figure 10 - Simplified sketch of sensor hole placement in test plate. All distances are in millimeters. The grayed area to the top left represents the approximate location of the tool at the end of the plunge.

With a zero degree head tilt the heating in the workpiece during the plunge is symmetric about the axis of the tool. This fact allowed sensors to be placed along a single plane out from the tool in simulation (as seen in Figure 11) and were placed in a radial pattern about the tool in experimentation (as seen in Figure 7).

Table 4 - Sensor positions used in testing.

Thermocouple Label	Radius from Tool Vertical Axis (mm)	Vertical Distance from Base of Workpiece (mm)
TC 1	0	0.5
TC 2	5	3
TC 3	6	6.5
TC 4	12	6.5
TC 5	15	6.5
TC 6	21	6.5
TC 7	27	6.5
TC 8	9	3
TC 9	12	3
TC 10	15	3
TC 11	21	3
TC 12	27	3

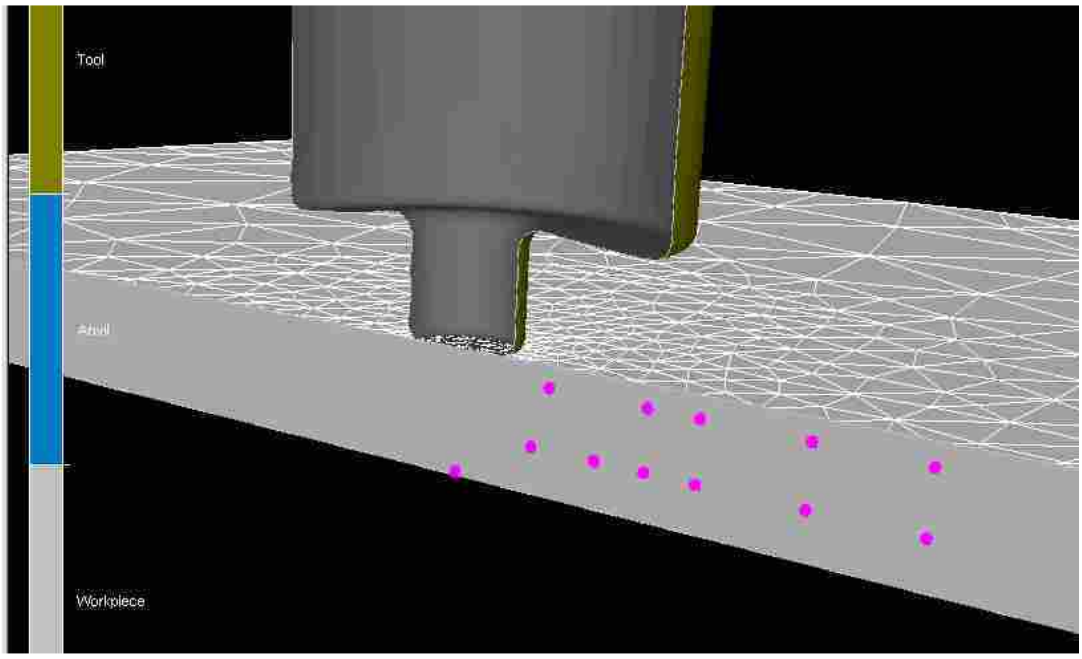

Figure 11 - Oblique screen shot of the linear placement of the sensors away from the tool in the workpiece.

3.2.4.Spindle Speed

Five simulations were completed varying the parameter of spindle speed. These five spindle speeds were 400, 500, 600, 700, 800 rpm.

3.2.5.Meshing

To tests the effect of mesh size three simulations were completed. Meshes are established in the workpiece by specifying concentric spheres. These meshes are centered at the intersection of the tool axis and the top surface of the plate. Concentric spheres are used to place the highest density of elements in the areas of the highest deformation and heating. Table 5 lists the parameters that defined the three mesh sizes. Included in the table is the number of nodes and elements in each simulated workpiece.

Table 5 - Selected mesh sizes and adjoining sphere sizes.

Coarse Mesh		Medium Mesh		Fine Mesh	
Mesh Region Radius (mm)	Mesh Edge Length	Mesh Region Radius (mm)	Mesh Edge Length	Mesh Region Radius (mm)	Mesh Edge Length
0 - 6	1.5	0 - 6	0.75	0 - 6	0.5
6 - 14	3	6 - 15	2	6 - 15	1
14 - 30	5	15 - 30	3	15 - 30	3
30+	15	30 - 40	8	30 - 40	7
		40+	15	40+	15
Nodes:	1,236	Nodes:	3,231	Nodes:	7,959
Elements:	4,532	Elements:	14,895	Elements:	39,974

3.2.6.Material Models

Forge2005 calculates flow stress as a function of strain, strain rate, and temperature. There are Forge2005 defined rheology equations, or the user can define a lookup table for flow stress.

Two basic material models exist in the Forge2005 database for aluminum 7075. These models are generally termed hot rheology and cold rheology. The hot rheology is stated to be valid in the region of strains .01 – 1 m/m, strain rate 0 – 200 m/ms, and temperatures 300 – 500°C. The cold rheology is stated to be valid in the region of strain .04 – 3 m/m, strain rate 0 – 500 m/ms, and temperatures 20 – 250°C. A conflict of the two valid regions occurs in the region of strains from .04 to .1 as seen in Figure 12; at specific strains the stress at 250°C is lower than at 300°C. This conflict prompted the testing of a user defined material model.

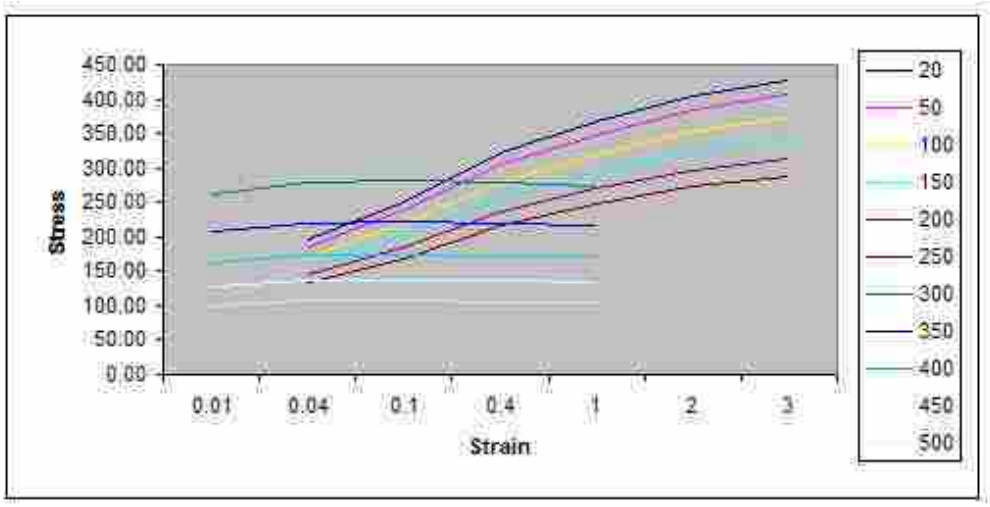

Figure 12 - Stress strain curves for the hot and cold material models as defined in Forge2005 at a strain rate of 100.

Lasley (2005) showed that a user defined material model could be used to improve the performance of the simulation in Forge2005. He determined that a good material model would be valid for strains 0 – 20, strain rates 0 – 500 s^{-1}, and temperatures 0 – 500^{o}C. Figure 13 and Figure 14 show maximum simulated strain and strain rate, respectively. The maximum strain is 20, and the maximum strain rate is 500 s^{-1}. The solidus temperature of AA 7075, 477^{o}C, gives an upper bound to the process temperature (Matweb, 2005).

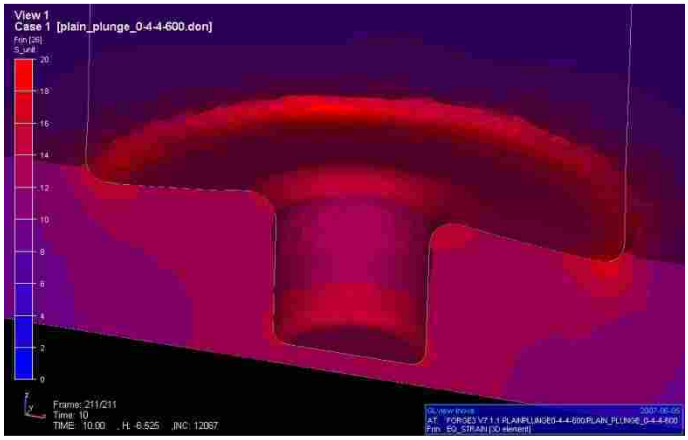

Figure 13 - Screenshot of equilateral strain values measured in each element at end of plunge.

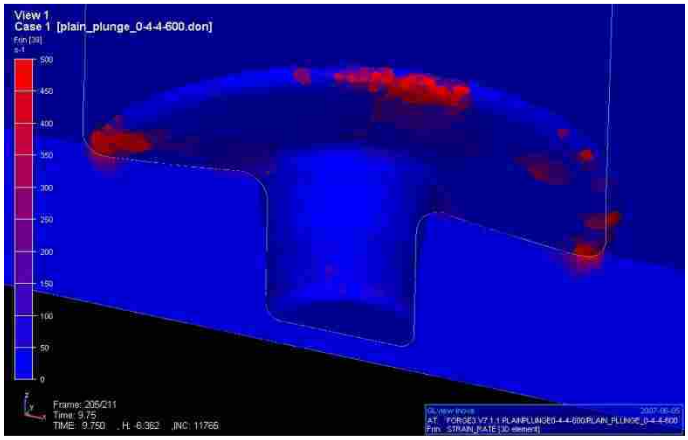

Figure 14 - Screenshot of strain rate values measured in each element at end of plunge.

The user defined material models are lookup tables where temperature, strain, and strain rate are used to determine stress. The user defined material models were variations of the cold and hot material models defined by Forge2005. The user defined material models provided a continuous set of values over the range of strain, strain rate, and temperature experience during a plunge and attempted to reconcile the differences of the hot and cold material models. The material models rh7, rh9, and rh10.

3.2.7. Thermal Exchange

The user is able to define thermal exchange between the tool and the workpiece. This value is constant during the course of a simulation. Forge2005 has four standard exchange values: adiabatic (0 W/m-K), mild (200 W/m-K), medium (1000 W/m-K) and strong (2000 W/m-K). These standard values were used in four simulations.

4. Results and Discussion of Results

Results of the plunge experiments were analyzed to show the influence of spindle speed variation and the behavior of the plunge during the dwell portion of the plunge process. Results of the simulations were analyzed to demonstrate the influence of the heat transfer coefficient and mesh size. Comparisons of the experimental results to the simulation results for identical spindle speed experiments is used to determine the comparable behavior, the influence of spindle speed, the significance of the heat transfer coefficient, and the influence of the material model on average temperature and temperature spread.

4.1. Plunge Experiments

Temperature results from the plunge experiments show notable behavior with variation in spindle speed and during the dwell following the plunge. The parameter of spindle speed is shown to have a definite but small effect on the temperature results. During the dwell, specific thermocouple positions reach equilibrium immediately following the conclusion of the plunge.

4.1.1.Spindle Speed Effect

Selected thermocouple data from all of the experiments was used to determine the influence of spindle speed on the workpiece temperature. As seen in Table 6 several thermocouples were removed from consideration. These run specific thermocouples were removed due to one of the following factors: no data returned by thermocouple, temperature results returned from an experiment that was not centered correctly, or incomplete insertion into the hole prohibited correct temperature records. Factors were determined by a temperature that was less than or greater than 20% of the paired value and less than or greater than 20% of the value approximation determined by the adjacent thermocouples in that run.

Table 6 –Thermocouples removed from consideration and the associated reason for removal. II indicates incomplete insertion; other labels are as indicated.

		Thermocouple											
Series	**Spindle Speed**	TC1	TC2	TC3	TC4	TC5	TC6	TC7	TC8	TC9	TC10	TC11	TC12
Set 1	400	<---------- ---------- Non Centered Experiment --------- ---------- ----->											
Set 1	500	No Data		II									
Set 1	600	No Data								II	II	II	
Set 1	700	No Data											
Set 1	800	No Data											
Set 2	400	No Data											
Set 2	500	No Data			II								
Set 2	600	No Data											
Set 2	700	No Data								II			
Set 2	800	No Data											

4.1.1.1. Results

Temperature values tended to increase as the spindle speed increased. Results for each of the locations show results similar to the representative result in Figure 15. Ten data points are

shown with one point for each of the experimental runs. A linear fit over the intervals reveals a positive slope for all measured values at all locations between four and eight seconds.

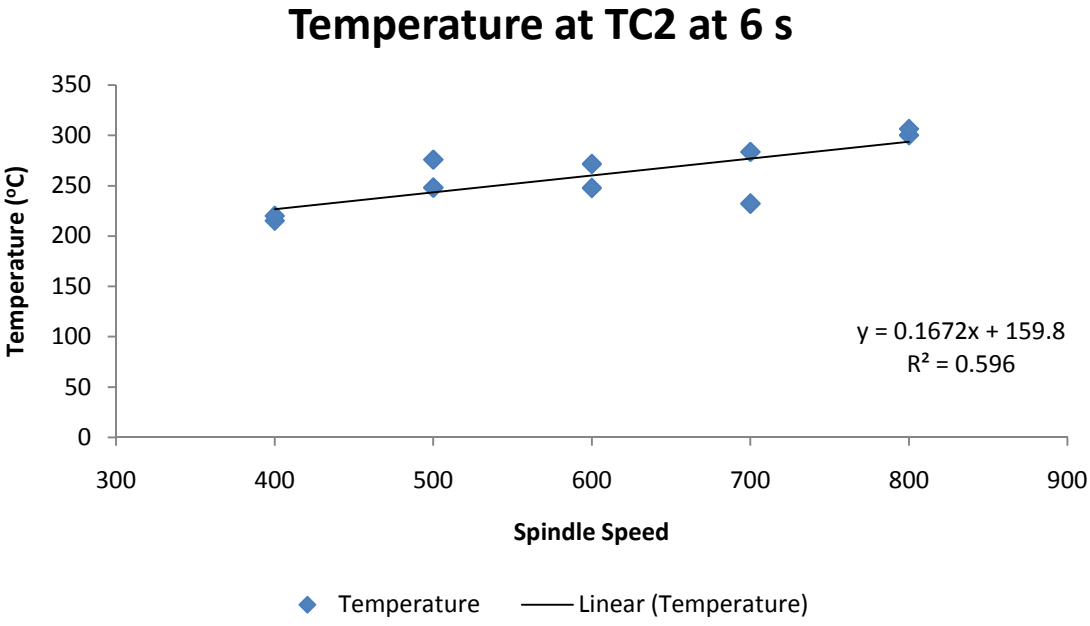

Figure 15 - Sample of the results of temperature at different spindle speeds at a fixed time and location.

4.1.1.2. Discussion of Results

The eleven thermocouples at 4, 6, 8 seconds at 5 spindle speeds are used to determine performance. A linear fit was applied to the potentially ten temperatures data points at each location, time, and speed triple. The resulting fit provided an approximate slope along with an associated f-statistic and number of degrees of freedom.

An f-test p-value was determined for each triple. p-values represent the probability that the observed variation resulted from a population with no correlation between spindle speed and

temperature. The resulting p-values are seen in Table 7 and indicate the confidence that there is no effect of spindle speed. 31 of 34 samples points at the points of 4, 6, and 8 seconds show with p-values of less than .05 the results did not occur by chance. This indicates that 31 of 34 are significant at the 95% confidence level. All points in the 4, 6, and 8 second time intervals have less than a .15 p-value. This result confirms the idea that an increase in spindle speed does have an effect on temperature.

Table 7 - P-values for each time location pair. Values determine through f-test at series of spindle speeds.

p value	Time		
TC Location	4	6	8
TC2	0.03	0.04	0.01
TC3	0.03	0.00	0.00
TC4	0.04	0.02	0.01
TC5	0.02	0.01	0.01
TC6	0.06	0.02	0.02
TC7	0.10	0.03	0.05
TC8	0.00	0.00	0.00
TC9	0.01	0.01	0.00
TC10	0.00	0.00	0.00
TC11	0.00	0.00	0.00
TC12	0.15	0.05	0.05

The coefficient consistently decreases as the radius increases. A plot of the linear slope approximation is seen in Figure 16 for the depths of 3 mm and 6.5 mm over the selected interval. Thermocouples closest to the tool experience a more significant change, 10-16 degrees per 100 rpm, than the more distant locations. This is in agreement with work in later sections showing that in the experimental work the heat does not transfer to the outside regions as quickly. This delayed dispersion prevents changes in spindle speed from having a significant impact in the more distant thermocouple locations.

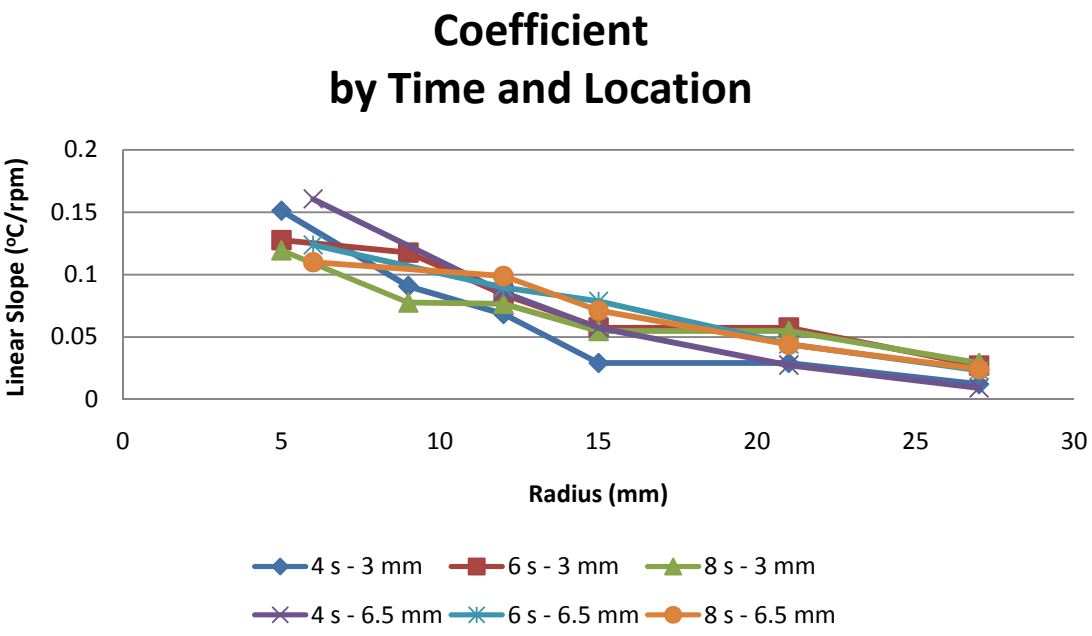

Figure 16 - Plot of associated linear slope for each time depth combination over the selected interval.

A change of spindle speed from 400 to 800 rpm would only increase temperature 40°C on average. Over the plunge duration temperature changes over 450°C. Thus a variation in spindle speed accounts for less than 10% of the total temperature change in the system.

4.1.2.Dwell Results

The temperature in the workpiece reaches equilibrium for some thermocouples in the time interval immediately following the plunge. The impact of the plunge dwell is one of the many parameters that could be examined in simulation modeling and experimentation. Thermocouples near the tool reach equilibrium almost immediately following the end of the plunge or the beginning of the dwell phase. The relative change in temperature during the dwell period indicates an equilibrium or transient state.

4.1.2.1. Results

General observations of the results of the plunge can be observed by noting the behavior of the eleven thermocouples placed in the material. The figures below show the results of the experimental plunge at the five plunge speeds (400 - Figure 17, 500 - Figure 18 , 600 - Figure 19, 700 - Figure 20, 800 - Figure 21). The z position is shown for the pin to clarify where the tool is plunging, dwelling, and extracting. There are three phases for each temperature curve. These phases match the approximate times of the plunge, shoulder impact, and dwell. However, for thermocouples more distant from the tool the response appears to be delayed. There is a temperature plateau for the thermocouples closest to the tool: TC2, TC3, and TC4.

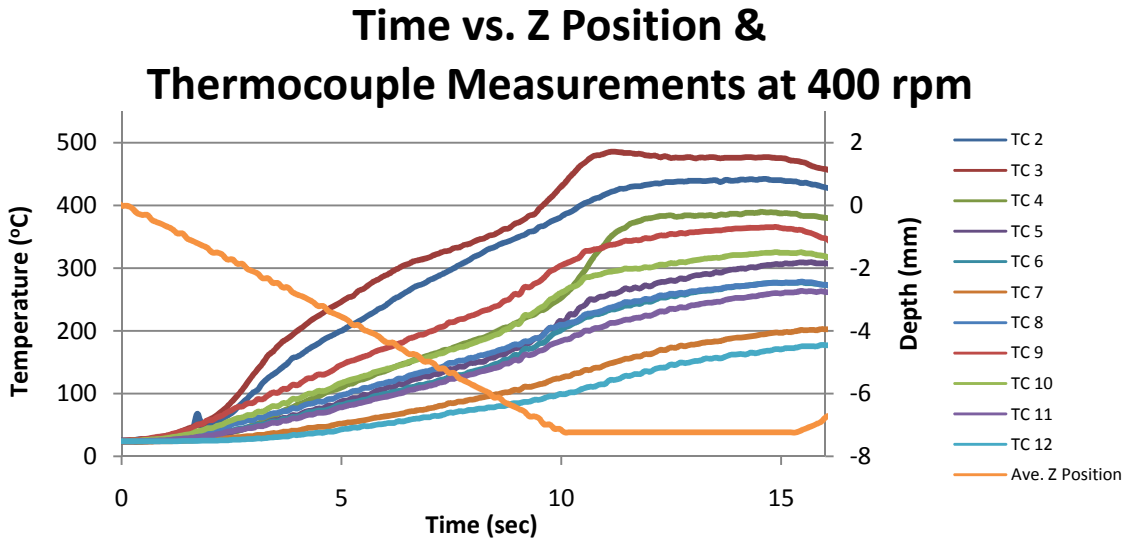

Figure 17- Plot of temperatures for experiment run with spindle speed of 400 rpm in time with secondary axis plot of tool position.

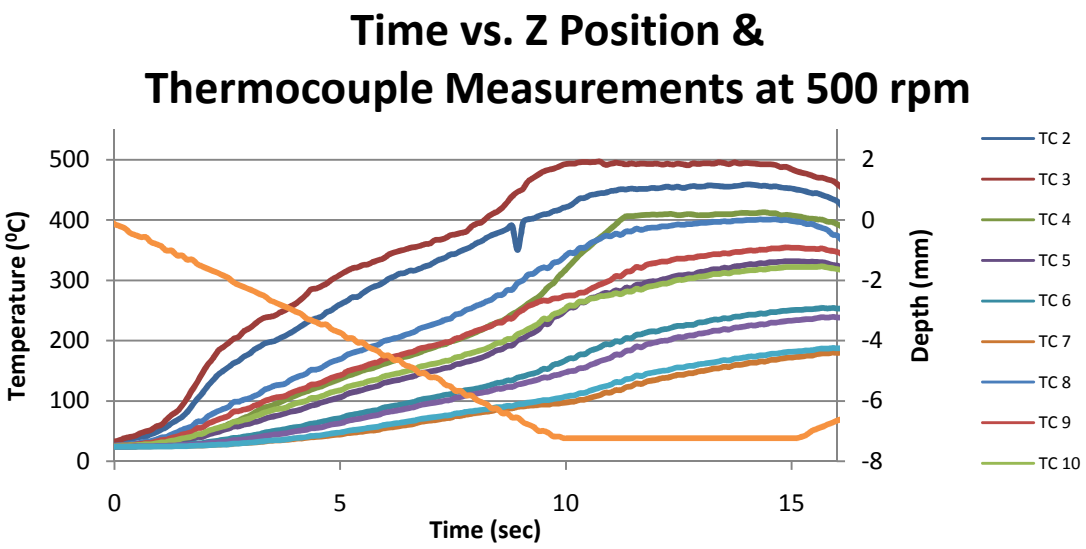

Figure 18 - Plot of temperatures for experiment run with spindle speed of 500 rpm in time with secondary axis plot of tool position.

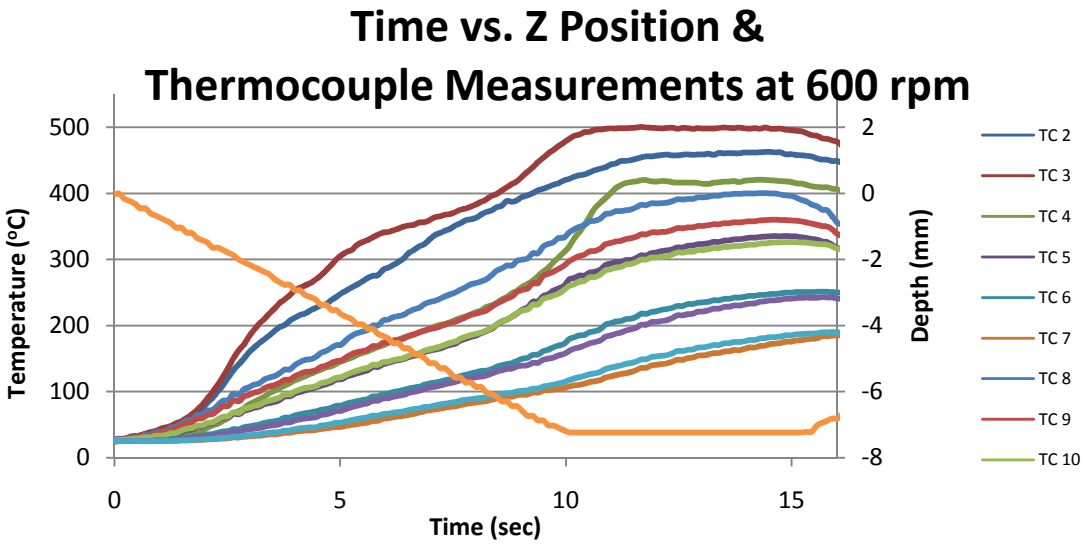

Figure 19 - Plot of temperatures for experiment run with spindle speed of 600 rpm in time with secondary axis plot of tool position.

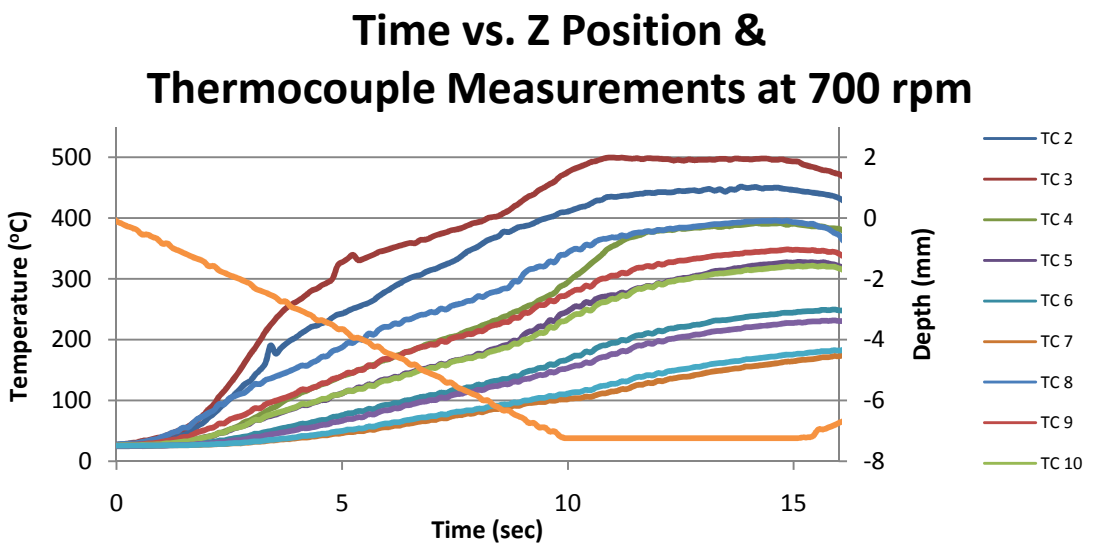

Figure 20- Plot of temperatures for experiment run with spindle speed of 700 rpm in time with secondary axis plot of tool position.

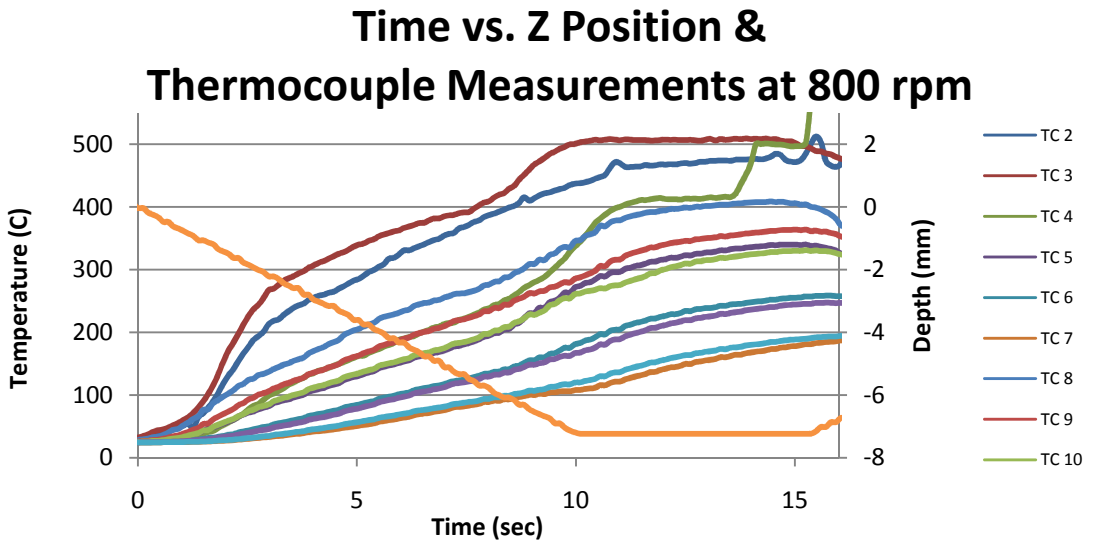

Figure 21- Plot of temperatures for experiment run with spindle speed of 800 rpm in time with secondary plot of tool position.

4.1.2.2. Discussion of Results

A linear slope comparison test is used to confirm that specific thermocouples experience a thermal plateau during the dwell portion of the plunge. The heating rate of the workpiece during the dwell is compared to the heating rate during the steady portion of the plunge. The dwell measurements are from 12.5 to 14.5 seconds where possible and between 11.5 and 13.5 in cases where the thermocouple was consumed in the experiment. i.e. TC 4 at a spindle speed of 800 rpm is consumed in the process. The measurements from the steady portion of the dwell are between 4 and 6 seconds. The ratio of the dwell heating rate to the plunge heating rate is used to evaluate if the thermocouple reaches thermal equilibrium. A ratio of zero constitutes equilibrium and a ratio of 1 constitutes equal heating rate in the dwell and plunge. The summary table of these results is seen in Table 8 and is plotted in Figure 22.

Table 8 - The heating rate ratio at each thermocouple locations at each spindle speed.

Heat Rate Ratio	Radius (mm)	400	500	600	700	800
TC 2	5	0.04	0.04	0.06	0.09	0.11
TC 3	6	0.00	0.03	0.00	0.02	0.05
TC 4	12	0.12	0.03	0.05	0.15	0.07
TC 5	15	0.56	0.55	0.45	0.48	0.37
TC 6	21	0.55	0.80	0.65	0.58	0.53
TC 7	27	0.94	1.65	1.44	1.10	1.13
TC 8	9	0.40	0.17	0.21	0.16	0.16
TC 9	12	0.19	0.33	0.30	0.26	0.29
TC 10	15	0.35	0.49	0.38	0.41	0.41
TC 11	21	0.65	0.90	0.78	0.56	0.62
TC 12	27	1.09	1.18	1.03	0.84	0.87

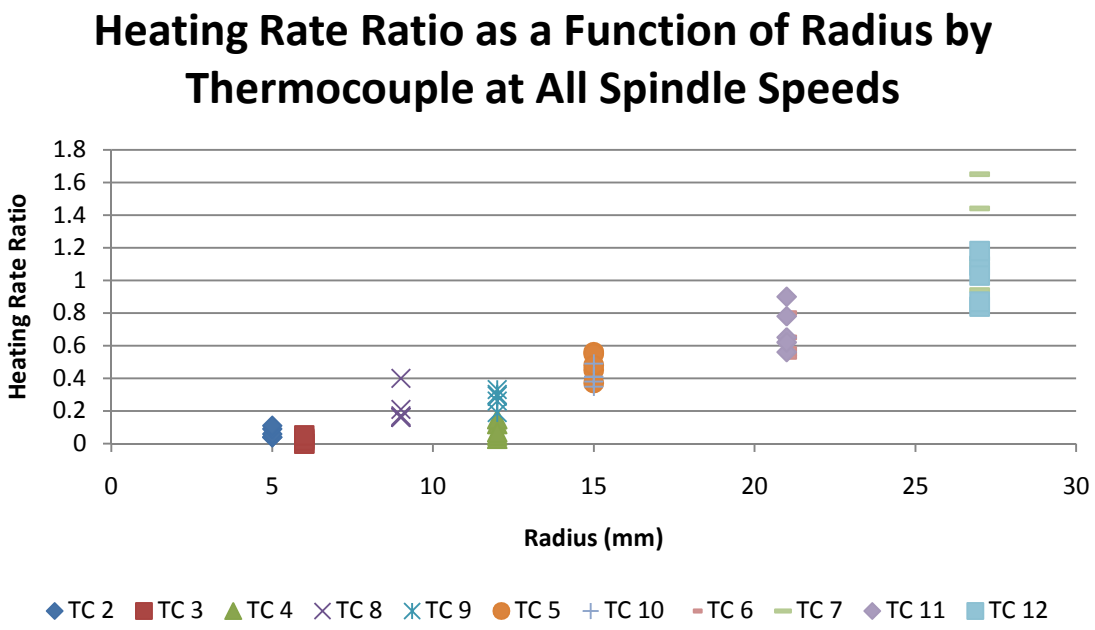

Figure 22 – Plot of heating rate ratio for thermocouple positions at all spindle speeds.

For TC2, TC3, and TC4 the heating rate ratios are consistently below 0.1 indicating a dramatic change between the two phases. For the locations of TC5, TC8, TC9 and TC10 the heating rate ratio varies between .15 and .50. The locations of TC6, TC 7, TC11, TC12 have a heating rate ratio greater than 0.65 and less than 1.2. For locations immediately adjacent to the tool the temperature immediately reaches a steady state, for locations most distant the dwell does not influence the behavior, and the intermediate regions slow but continue temperature rise.

4.2. Forge2005 Simulations

Simulation results use sensor temperatures to show the influence of mesh size and heat transfer coefficient. Models with three different mesh sizes were simulated and used to give guidance in the selection of mesh size to balance duration and temperature change. Four heat

transfer coefficients were used to define a relationship relating increase in heat transfer coefficient and decrease in temperature from the adiabatic condition.

4.2.1.Mesh Size Influence

4.2.1.1. Results

Temperature in the workpiece decreases with increasing mesh size. Mesh size is potentially a function of several variables but for simplification the number of nodes in the workpiece will be the measure used here. Plots of the temperature results of the simulations at 4, 6, and 8 seconds are found below in Figure 23, Figure 24, and Figure 25. A reduced number of sensors were used to simplify calculations.

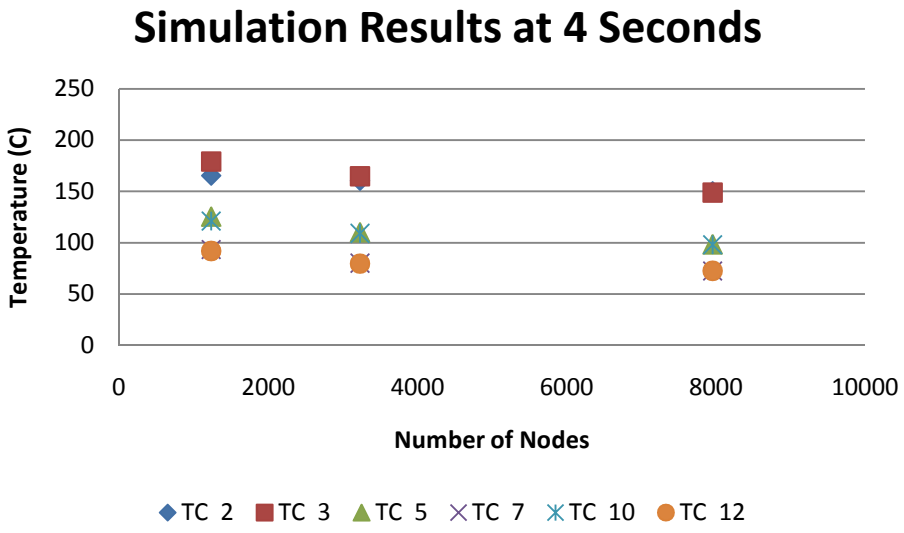

Figure 23 - Plot of simulation results at 4 seconds for three mesh sizes at 6 thermocouple locations.

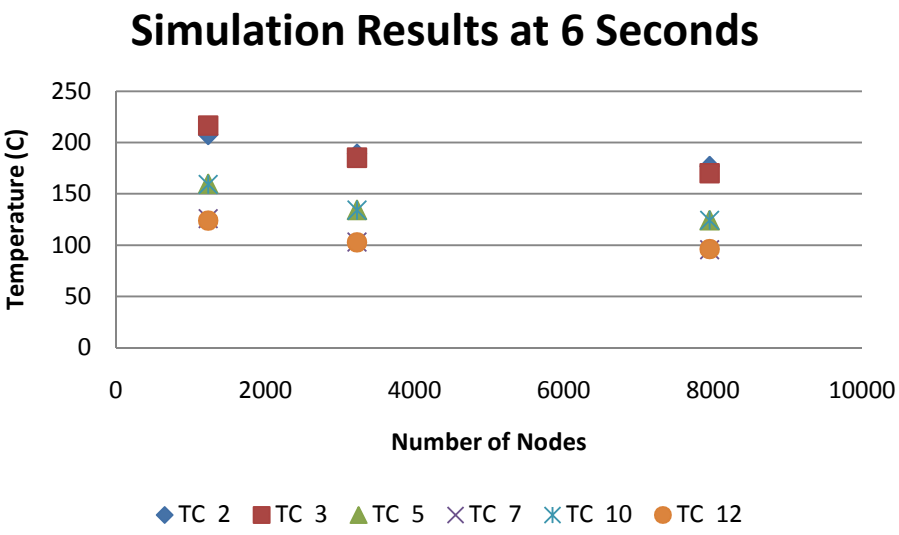

Figure 24 - Plot of simulation results at 6 seconds for three mesh sizes at 6 thermocouple locations.

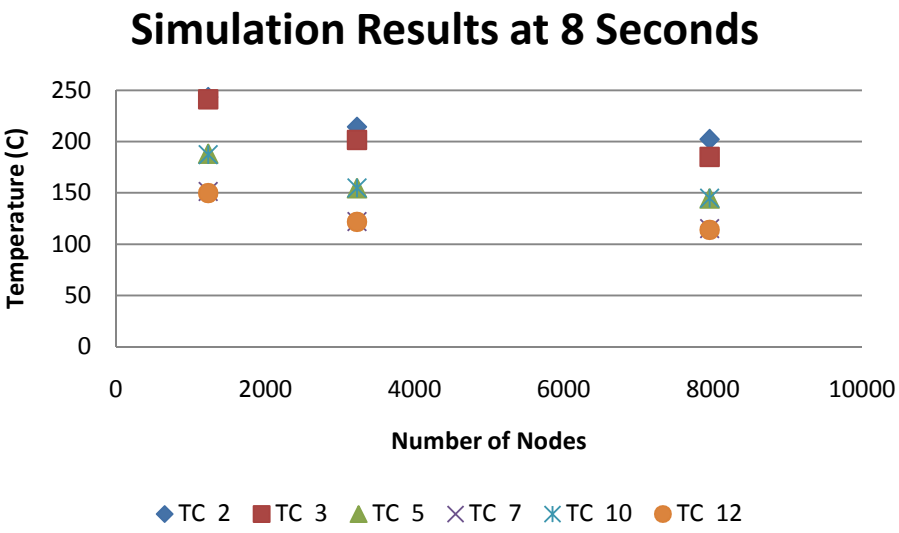

Figure 25 - Plot of simulation results at 8 seconds for three mesh sizes at 6 thermocouple locations.

4.2.1.2. Discussion of Results

There is a diminishing decrease in temperature for addition mesh detail. A power curve is used to approximate the behavior. The general equation model followed has the following format:

$$f(x) = a * x^b + c \tag{1}$$

A regression was used to simultaneously determine each series' horizontal asymptote and the shape of the curve that fit through the data series. A common value for a and b is determined to give the same shape of curve through each of the resulting values. A variable c is used to account for the different radial distances of each thermocouple. This resulting function is:

$$f(x) = 11725 * x^{-0.788} + c. \tag{2}$$

Where c is the individual data series horizontal asymptote value. Values of the horizontal asymptotes are seen in Table 9. The horizontal asymptote is used to represent the temperature under when an infinitely fine mesh is used.

Table 9 - Horizontal asymptotes for simultaneous solutions of curve fit method.

Time/Location	TC2	TC3	TC5	TC7	TC10	TC12
4	140.	134.	85.	85.	58.	58.
6	166.	166.	115.	115.	83.	83.
8	196.	184.	138.	138.	104.	104.

Using the horizontal asymptote as the final temperature value for each data series, the amount of the reduction in error to the final value can be determined for each mesh size. The

percent of change from the horizontal asymptote was determined for each data point and average at each mesh size. This is called the percent over-approximation and the calculation is the equation

$$Over\ Approximation\ (\%) = \frac{(\theta_{sensor} - \theta_{asymptote})}{\theta_{asymptote}}. \quad (3)$$

The result of the calculations is plotted in Figure 26.

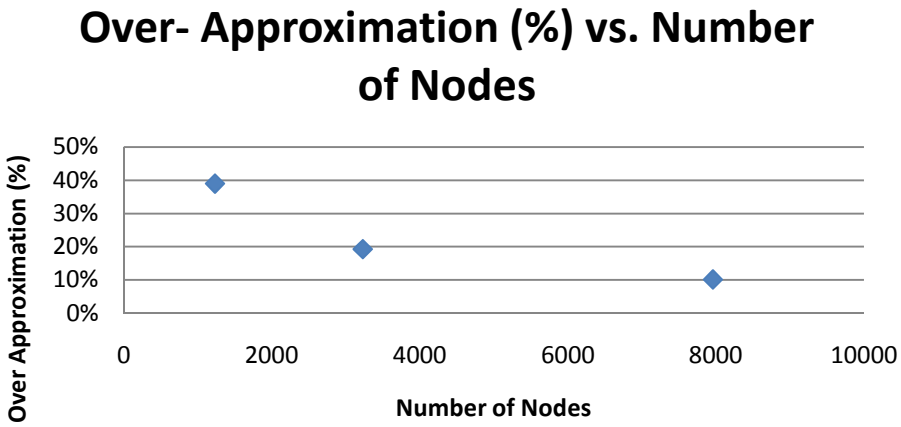

Figure 26 - Plot of the over-approximation (%) at selected times and locations against the number of nodes.

Using the number of computation hours required to complete the simulation from Table 10 a plot of the over-approximation percent is seen below in Figure 27. In order to balance the number of hours required to complete a simulation and the change in the temperature a compromise is made between the two factors. The medium mesh size shows 20% over-approximation and that doubling the computation time only improves the over approximation to 10%. A medium mesh size should be sufficient for most friction stir plunge simulations.

Table 10 - Number of elements, number of nodes, and computation time by mesh size.

	Coarse Mesh	Medium Mesh	Fine Mesh
Number of Elements	4,532	14,895	39,974
Number of Nodes	1,250	3,200	8,000
Computation Time	42 hrs.	180 hrs.	370 hrs.

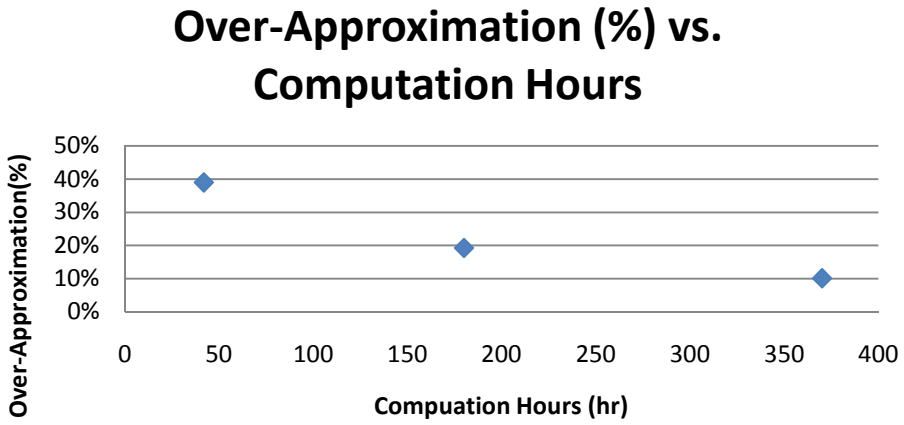

Figure 27 - Plot of the over-approximation (%) at selected times and locations against the number of computation hours.

4.2.2. Heat Transfer Coefficient Influence

The heat transfer coefficient consistently decreases temperature in the workpiece as the coefficient value increases. This parameter regulates the interaction between the tool and the workpiece in the simulation and provides a means for heat to move out of the workpiece. The influence of the heat transfer coefficient on temperature can be determined by a series of simulations that vary this parameter. The percent change in temperature as the heat transfer coefficient is increased from zero offers a single measure of this effect.

4.2.2.1. Results

The adiabatic model has the highest temperature across all simulations as seen in Figure 28. The adiabatic model has a heat transfer coefficient of zero and indicates that all heat will be retained inside the workpiece with the parameter value. This lower limit acts as a boundary condition and reference point for all other simulations. The other simulation models have lower temperatures at all locations and decrease in temperature as the heat transfer coefficient increases.

The locations of TC2, TC3, TC5, TC7, TC10, and TC12 are used for evaluation. Analysis is performed at the times of 4, 6 and 8 seconds.

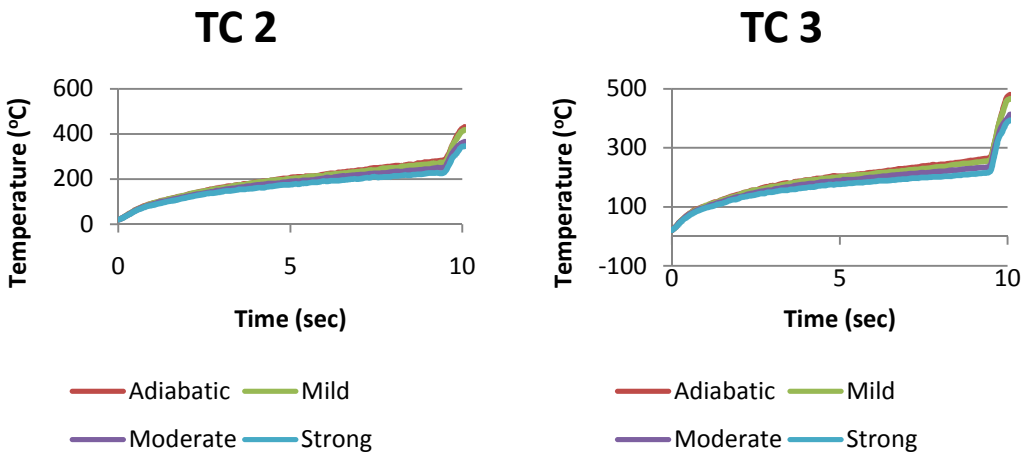

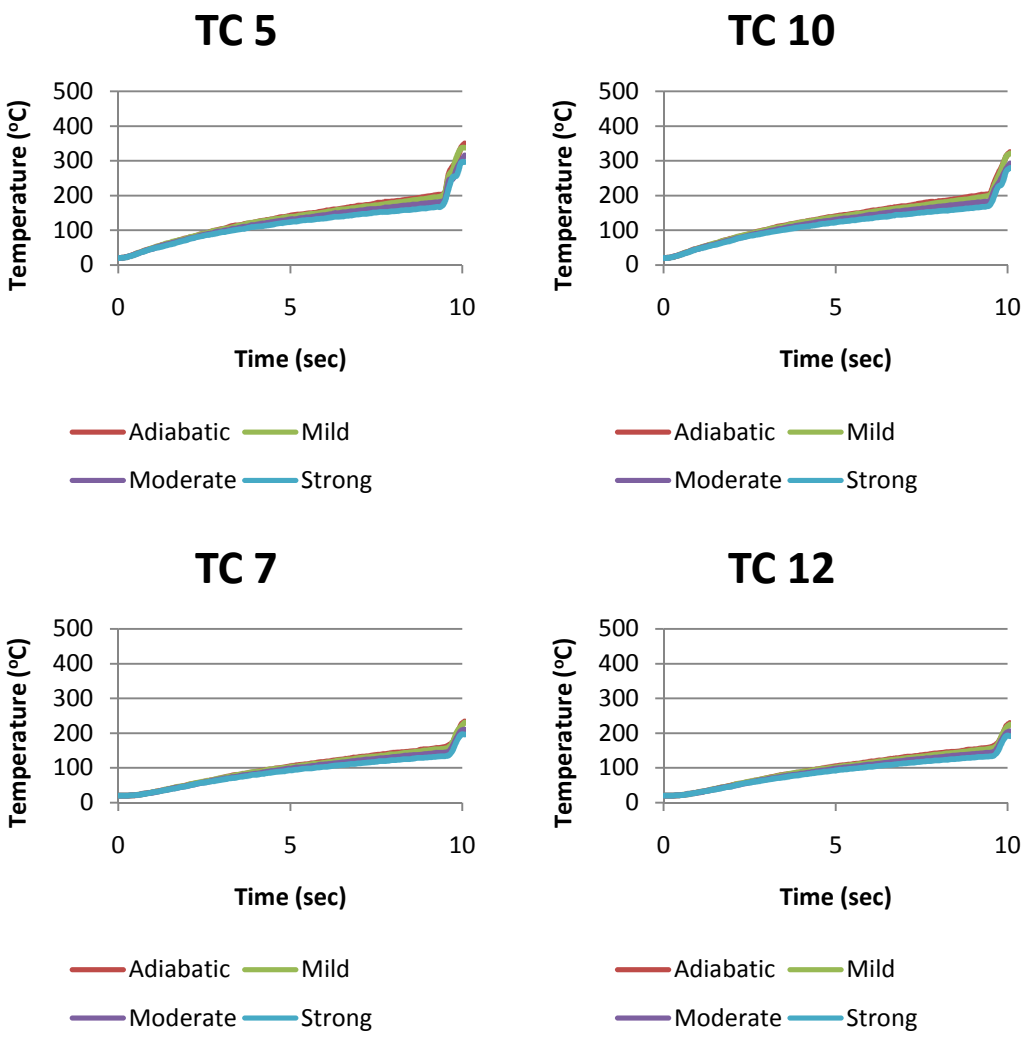

Figure 28 - A series of plots that show the temperature curves for four different heat transfer coefficents at six selected locations.

4.2.2.2. Discussion of Results

Using this natural boundary, change from the known limit can indicate trends in behavior. As temperature is the recorded measure a percent change in temperature from the adiabatic value here called adiabatic change is determined for all points in the selected interval.

The adiabatic change can be influenced by the heat transfer coefficient, the sensor position, and time. A plot of the results at TC2 is seen in Figure 29, the influence of sensor position and time is less than 4% change each or less than 20% of the total change. The equation can then be simplified so that the percent decrease from adiabatic is only a function of the heat transfer coefficient.

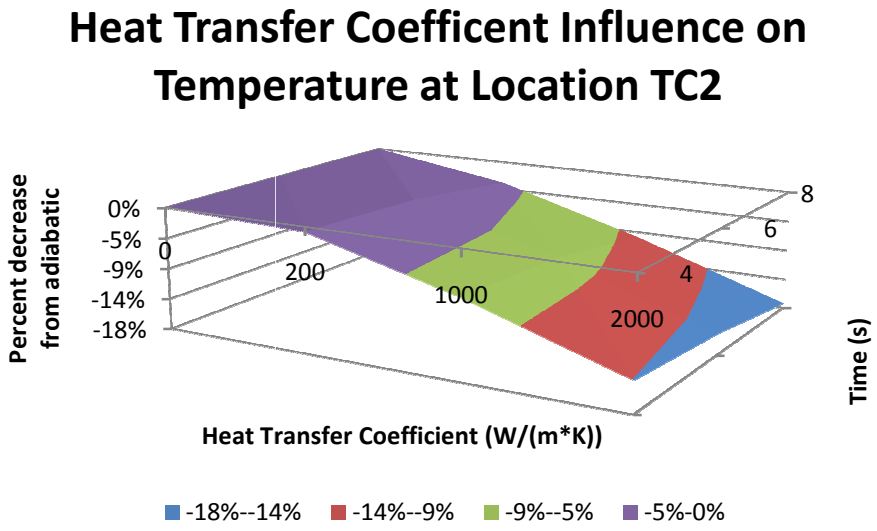

Figure 29 - Series of figures demonstrating the percent change in temperature from the adiabatic value according to the time (sec) and heat transfer coefficient.

The average percent change from the adiabatic temperature over the interval for the tested heat transfer coefficients gives a reasonable approximation of the influence of the parameter on the workpiece temperature. A linear approximation of the average percent change in temperature as a function of the heat transfer coefficient is:

$$\Delta\theta = -7x10^{-5} * \left(Heat\ Transfer\ Coefficent\ \left(\frac{W}{mK}\right)\right) \quad (4)$$

The plot of the data and resulting fit is seen in Figure 30. The R^2 value of .92 shows the linear approximation fits the data reasonably well. This formula result indicates that for every 1000 W/m-K increase in the heat transfer coefficient between the tool and the workpiece the temperature drops 7% from the adiabatic value.

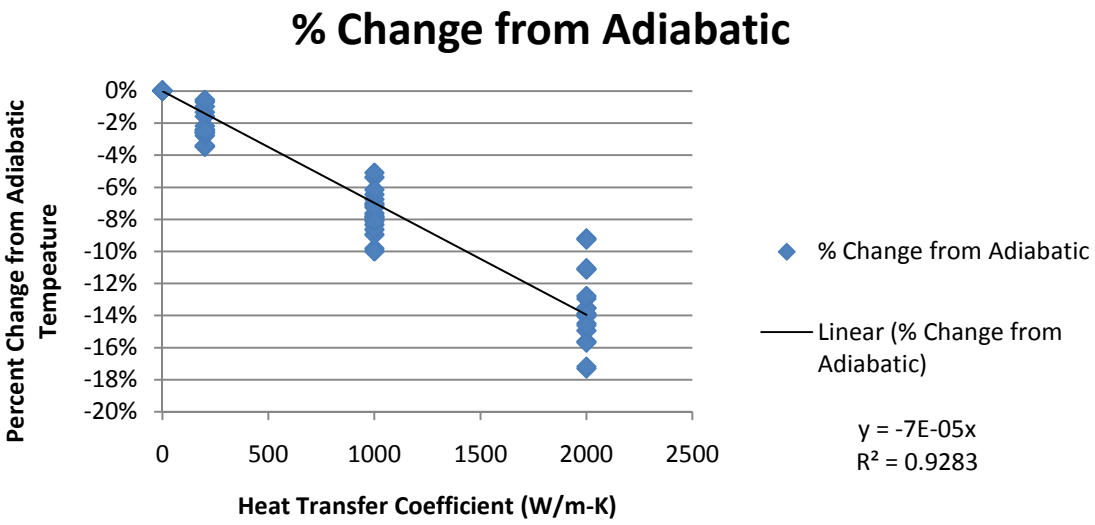

Figure 30 - Plot of percent change in temperature from adiabatic temperature as the heat transfer coefficient increases.

4.3. Comparison

The changes of simulation parameters have the most relevance when compared with the experimental results. Both the simulation temperature curve and the experiment temperature curve behavior move in similar but distinct patterns. Spindle speed shows similar temperature change. The significance of the heat transfer coefficient in influencing temperature is shown to be small relative to the other changes in the system. The material model influence is demonstrated to

be ineffective matching the temperature spread of the experiment and partially effective in determining average temperature.

4.3.1. General Comparison of Temperature Curves

4.3.1.1. Results

The comparison of the experimental temperature results and the basic simulations temperatures uses the locations of TC2 and TC12. To validate that the simulation temperature curves are not solely a function of the parameter selection several simulation temperatures were simultaneously compared to the experimental temperatures. The standard simulation is a hot material model, strong heat transfer coefficient, and a medium mesh. Also plotted is a variation using the user defined material model rheology 9 (MM rh9), a variation with mild heat transfer between the tool and workpiece (HT mild), and a variation with a fine mesh size (MS fine). The parameters used are shown in Table 11. Figure 31 and Figure 32 below show comparison plots for the experiment at a spindle speed of 600 rpm as compared with several variations of simulation all at a spindle speed of 600 rpm.

Table 11 - Various simulation models used in comparison to experiment.

Label	Spindle Speed	Material Model	Heat Transfer Coefficient	Mesh Size
Standard	600	Hot	Strong	Medium
MM rh9	600	rh9	Strong	Medium
HT mild	600	Hot	Mild	Medium
MS fine	600	Hot	Strong	Fine

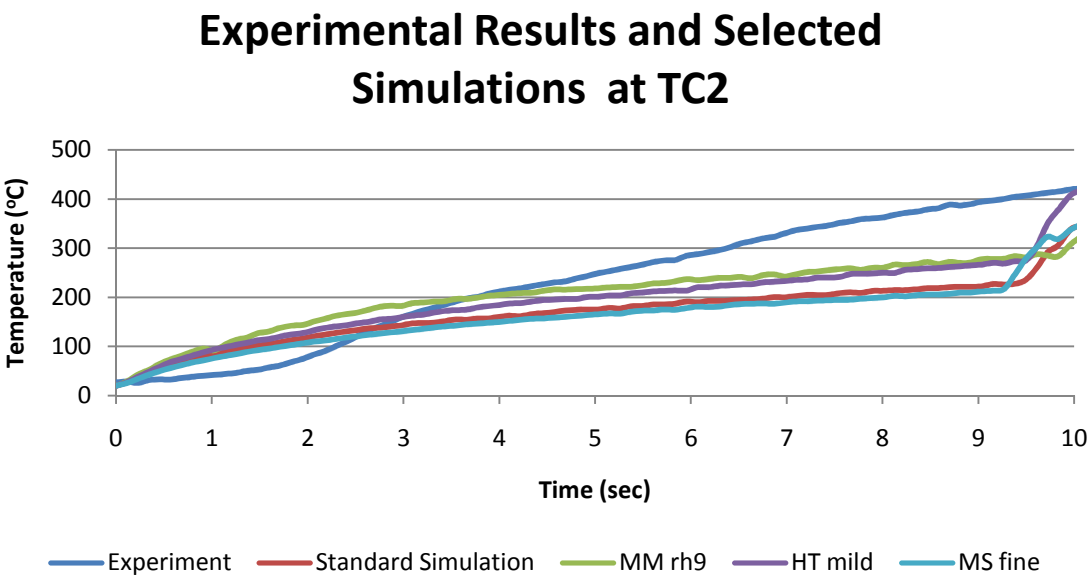

Figure 31 - Comparison plot of experimental and selected simulation models at thermocouple location TC2.

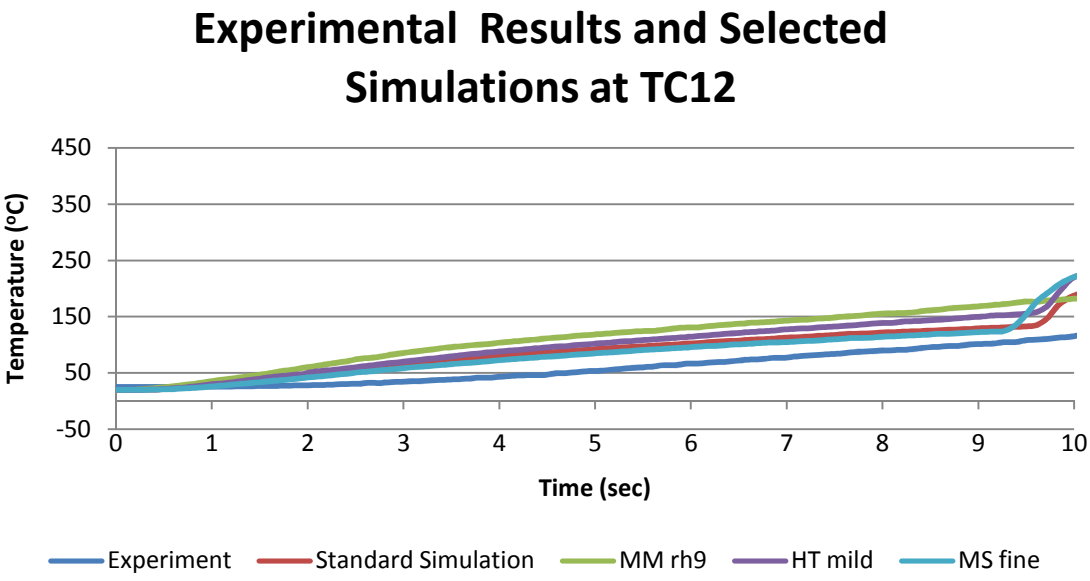

Figure 32 - Comparison plot of experimental and selected simulation models at thermocouple location TC12.

All measured temperatures follow the gradually increasing trend observed in the plots. All simulations experience a sharp rise in temperature as the shoulder of the tool contacts the workpiece around 9.5 seconds. Simulation experiments tend to parallel one another in rise.

4.3.1.2. Discussion of Results

A central slope at was taken for each time by considering a central difference over a from 0.5 to 8.5 seconds to generate the heating rate. The results are seen in Figure 33 and Figure 34. The heating rate remains consistent in all cases after 4.5 seconds. After the heat input reaches the thermocouple location there is a steady increase in temperature indicating a constant heat applied at this location. The simulation temperature slope falls off at an exponential rate from the start of the simulation. This exponential curve matches the behavior of the exponential functions found in Forge2005 that define the heat interactions within the workpiece (Transvalor, 2005). The behavior the experiment and the simulation are shown to be different by considering the heating rate.

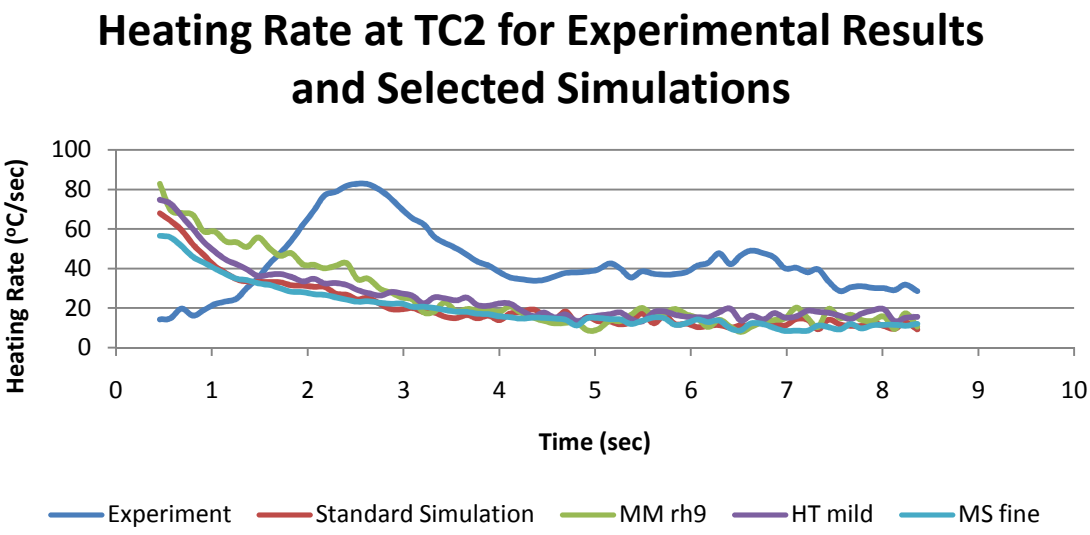

Figure 33 - Plot of approximated slope for experimental temperatures and experimental temperatures for selected simulation models at thermocouple and sensor location TC2.

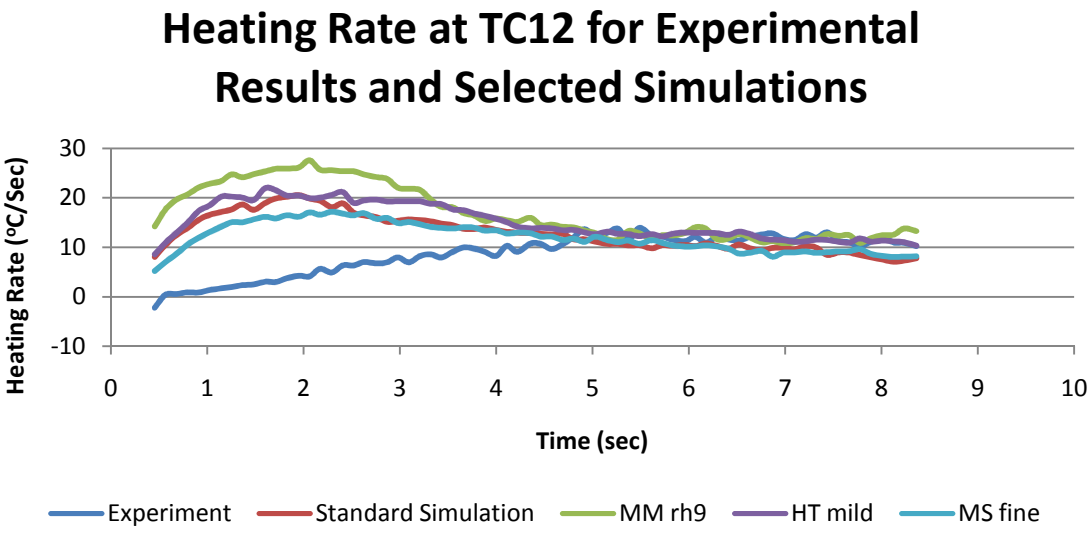

Figure 34 - Plot of approximated slope for experimental temperatures and experimental temperatures for selected simulation models at thermocouple and sensor location TC12.

4.3.2. Comparative Spindle Speed Influence

4.3.2.1. Results

Results from the simulation and experiment were collected at the locations of TC2 and TC12 for all five spindle speeds. Plots of the simulation temperature curves are seen in Figure 35, Figure 36, and plots of the experimental temperature curves are seen in Figure 37, and Figure 38. All plots show that 400 rpm is the coolest temperature and 800 rpm is the warmest at the inner-most and outer-most locations.

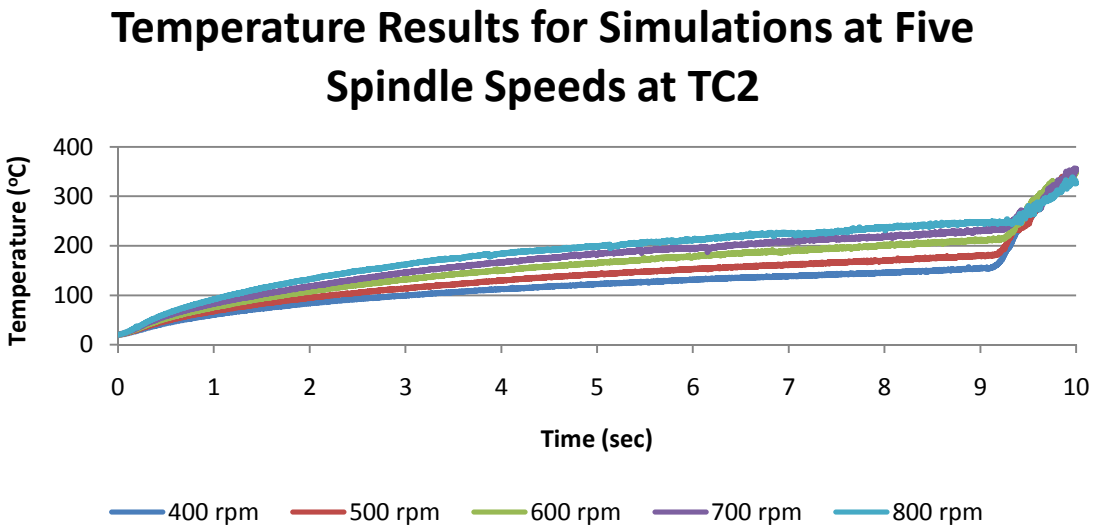

Figure 35 - Plot of temperature results in simulation at TC2 for five spindle speeds.

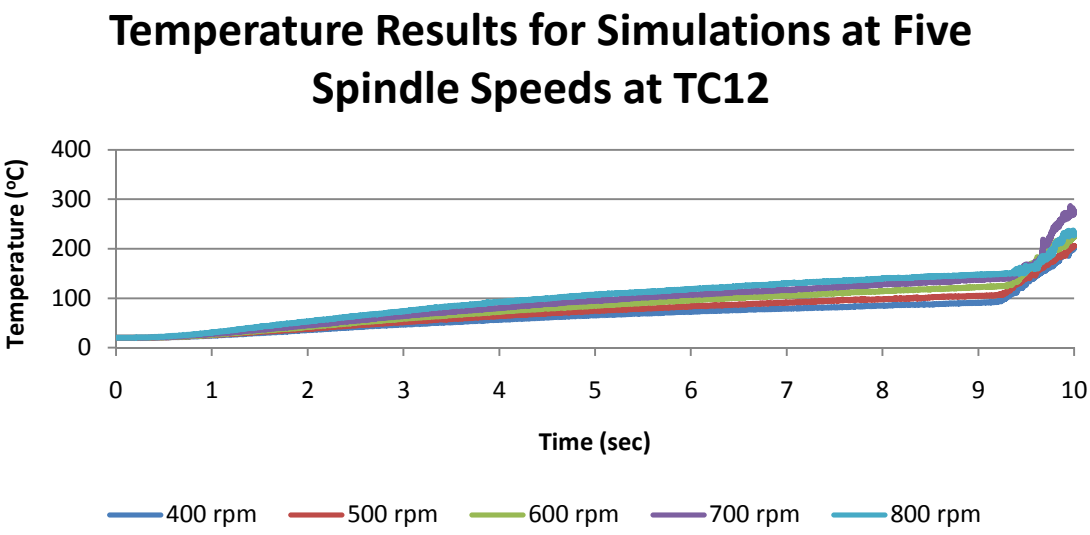

Figure 36 - Plot of temperature results in simulation at TC12 for five spindle speeds.

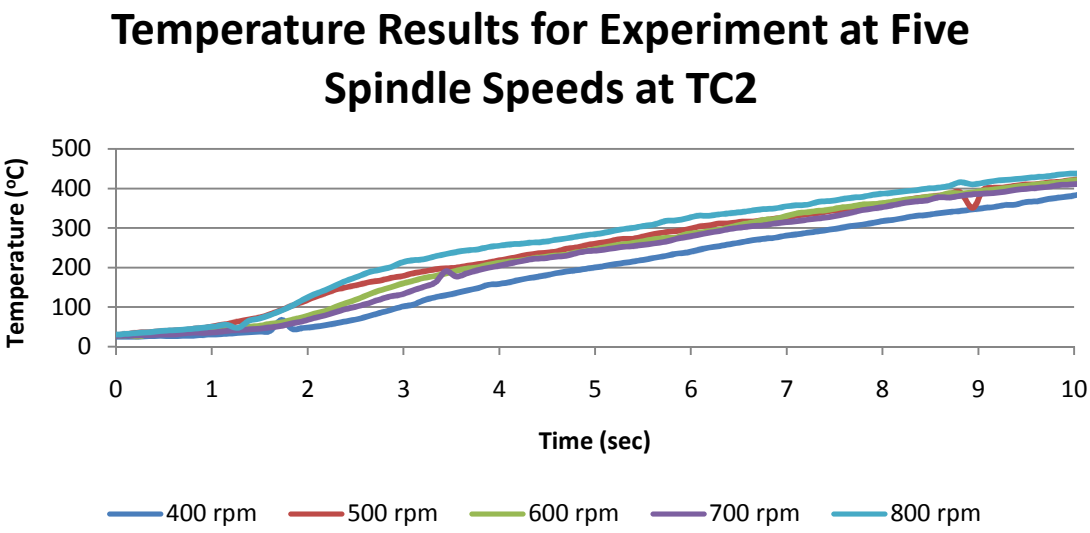

Figure 37 - Plot of temperature results in experimentation at TC2 for five spindle speeds.

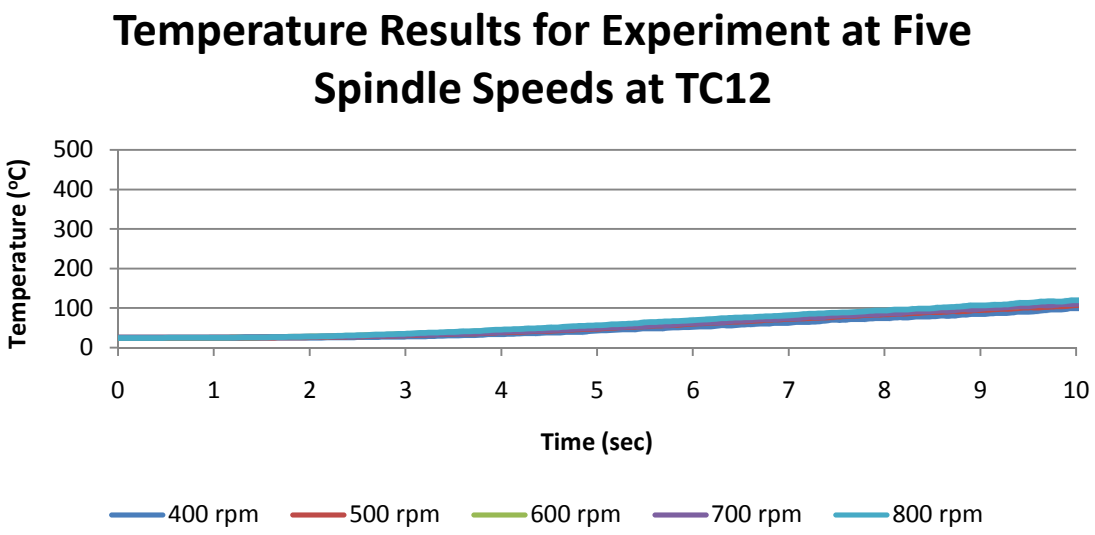

Figure 38 - Plot of temperature results in experimentation at TC12 for five spindle speeds.

4.3.2.2. Discussion of Results

A coefficient is determined at 6 seconds to compare the experimental and simulation values. Figure 39 and Figure 40 show that the experiment temperatures are higher than the simulation temperature closer to tool and lower further from the tool. The coefficient is determined by a linear fit of the points. The simulation coefficient is larger than the experimental coefficient at both locations. Both the experiment and simulation show that with increase spindle speed the temperature in the workpiece increases.

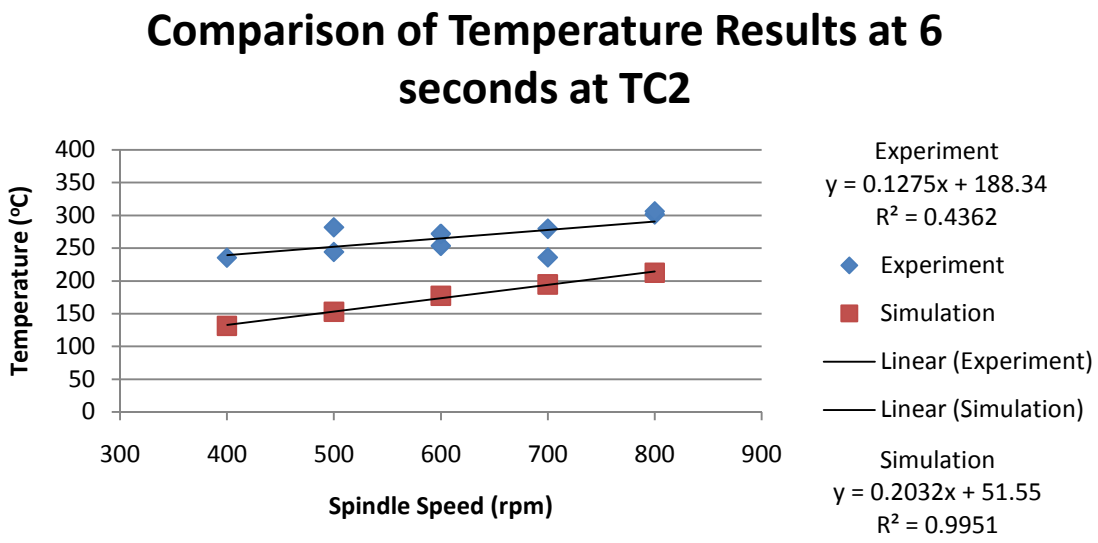

Figure 39 - Comparison of temperatures at 6 seconds between simulation results and experimental results. at TC2.

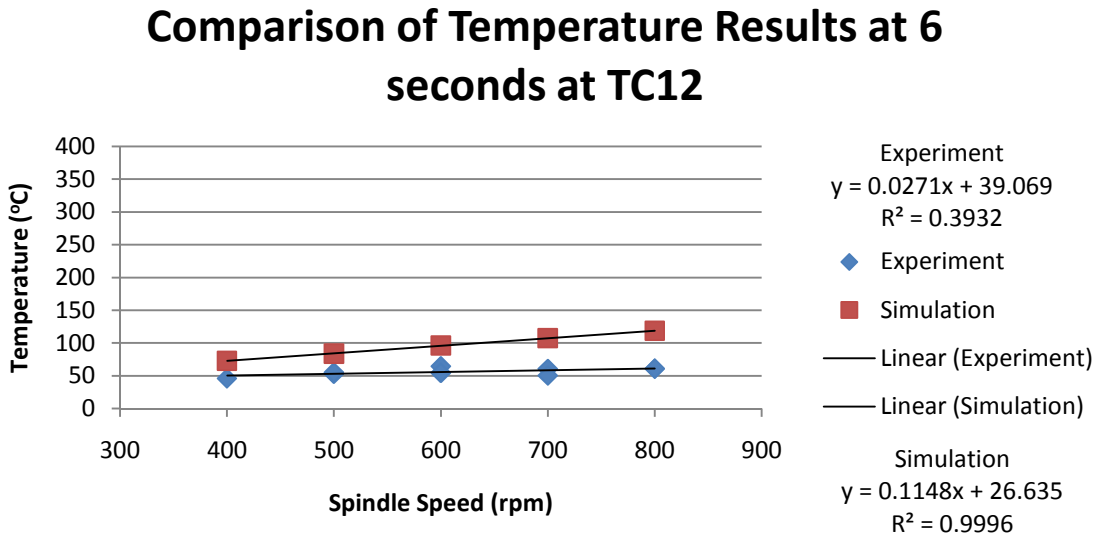

Figure 40 - Comparison of temperatures at 6 seconds between simulation results and experimental results. at TC12.

Comparison of the coefficient as a function of radius shows the similarities of the experiment and simulation. As seen in Figure 41 the simulation coefficient varies from .21 to .11. The experimental coefficient varies from .12 to .03. Both curves drop .09 over the interval. This parallel drop shows that the spindle speed influence as a function of radius matches between the simulation and the experiment.

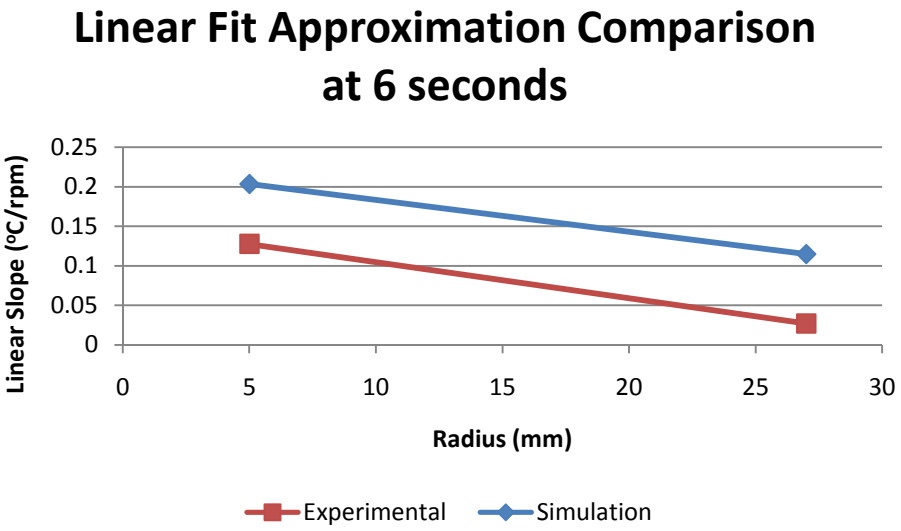

Figure 41 - Comparisons of linear slope at a depth of 3mm between simulation slope and experimental slope at two locations, TC2 and TC12.

4.3.3. Heat Transfer Coefficient Significance

4.3.3.1. Results

Simulation curves with a variable heat transfer coefficient as compared to the experimental curve at the same spindle speed show distinctly different behavior. The

experimental results appears to be consistently increasing in temperature over the course of the plunge. The simulations however show a consistent region during the main portion of the plunge but show a dramatic change when the shoulder of the tool reaches the surface of the workpiece. The simulation temperature does draw closer to the experimental temperatures at the close of the simulation in the TC 2, TC 3, TC 5, and TC 10 positions. However, the simulations do not match models of the experiemental temperatures through the bulk of the simulation at the TC 2, TC 3, TC 7, and TC 12 locations, as seen in the array of figures below as Figure 42.

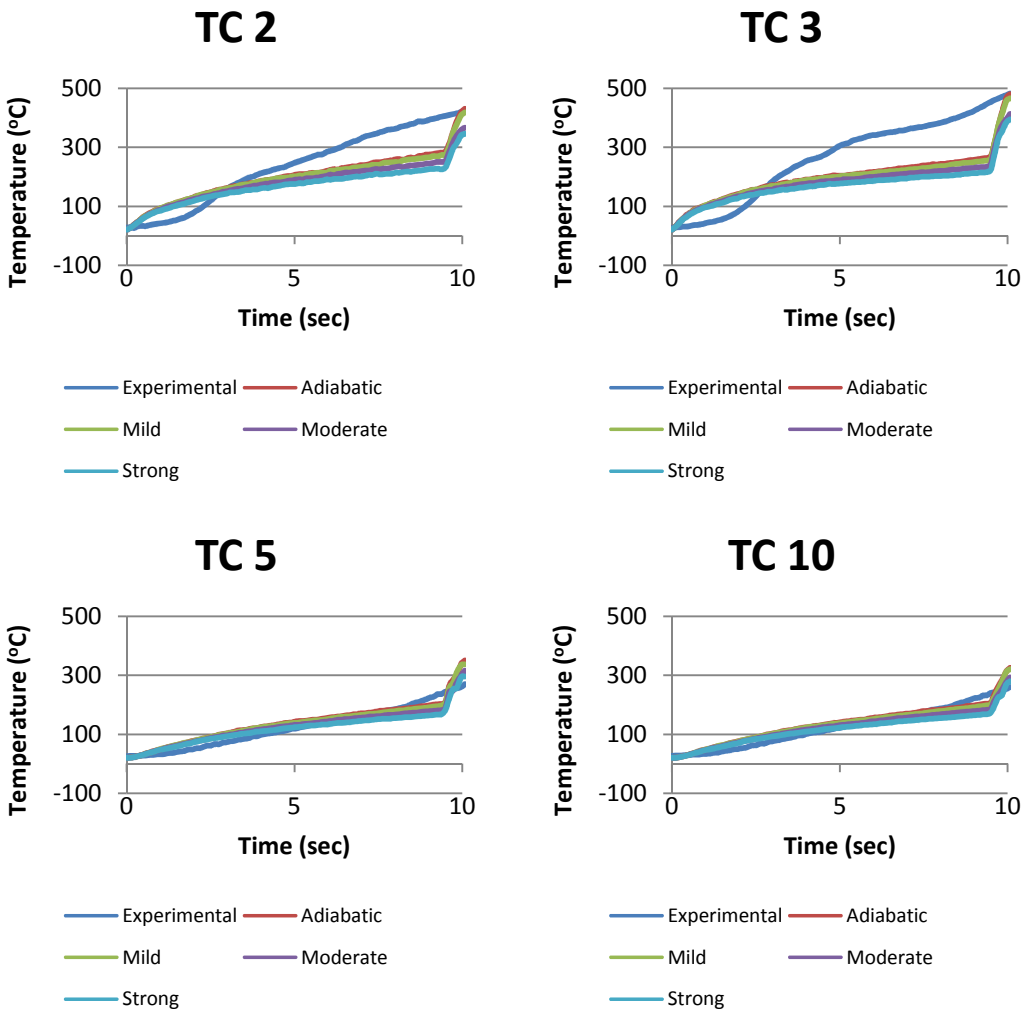

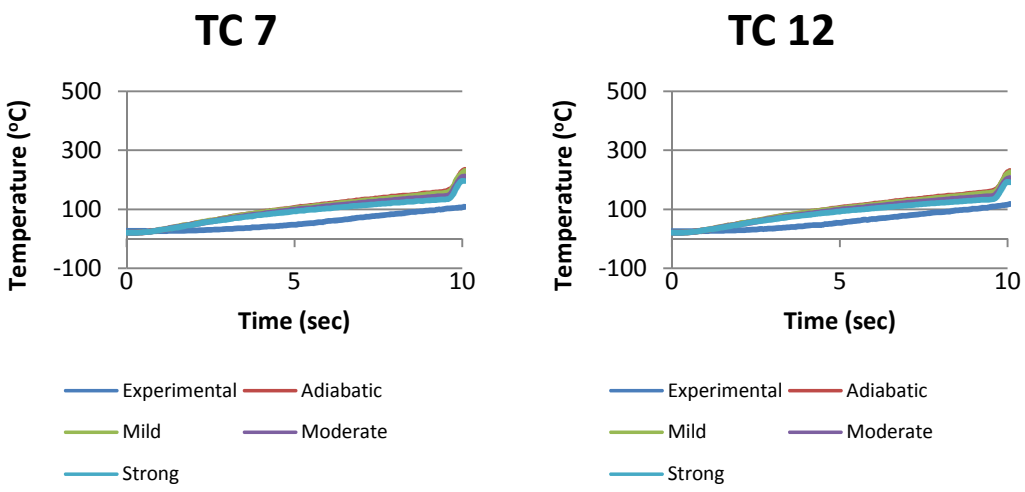

Figure 42 - Series of plots showing temperature results for experiment and series of simulations with different heat transfer coefficients at various locations.

4.3.3.2. Discussion of Results

Observation of Figure 42 shows that the simulations with variable heat transfer tend to be closely grouped together. The experimental temperatures vary significantly by time and location and do not follow the same general shape as the other data curves. A comparison where the experimental temperature is used as the reference would allow the generalizations of the behavior of all of the simulations to be better understood. This comparison is seen in Figure 43.

There are two key observations. First, the simulation results are almost identical in all locations through all times; varying by less than 80°C in the most extreme instance at a location. Second, the experimental temperatures vary significantly from the simulation temperatures, over 200°C between locations, and vary in rate of increase. For the location of TC2 it is noted from Figure 42 the total rise in the experiment is over 400°C and in Figure 43 the maximum change between the adiabatic heat transfer and the strong heat transfer is <80 °C. These values indicate less than 20% of the total change in temperature can be attributed to the heat transfer coefficient.

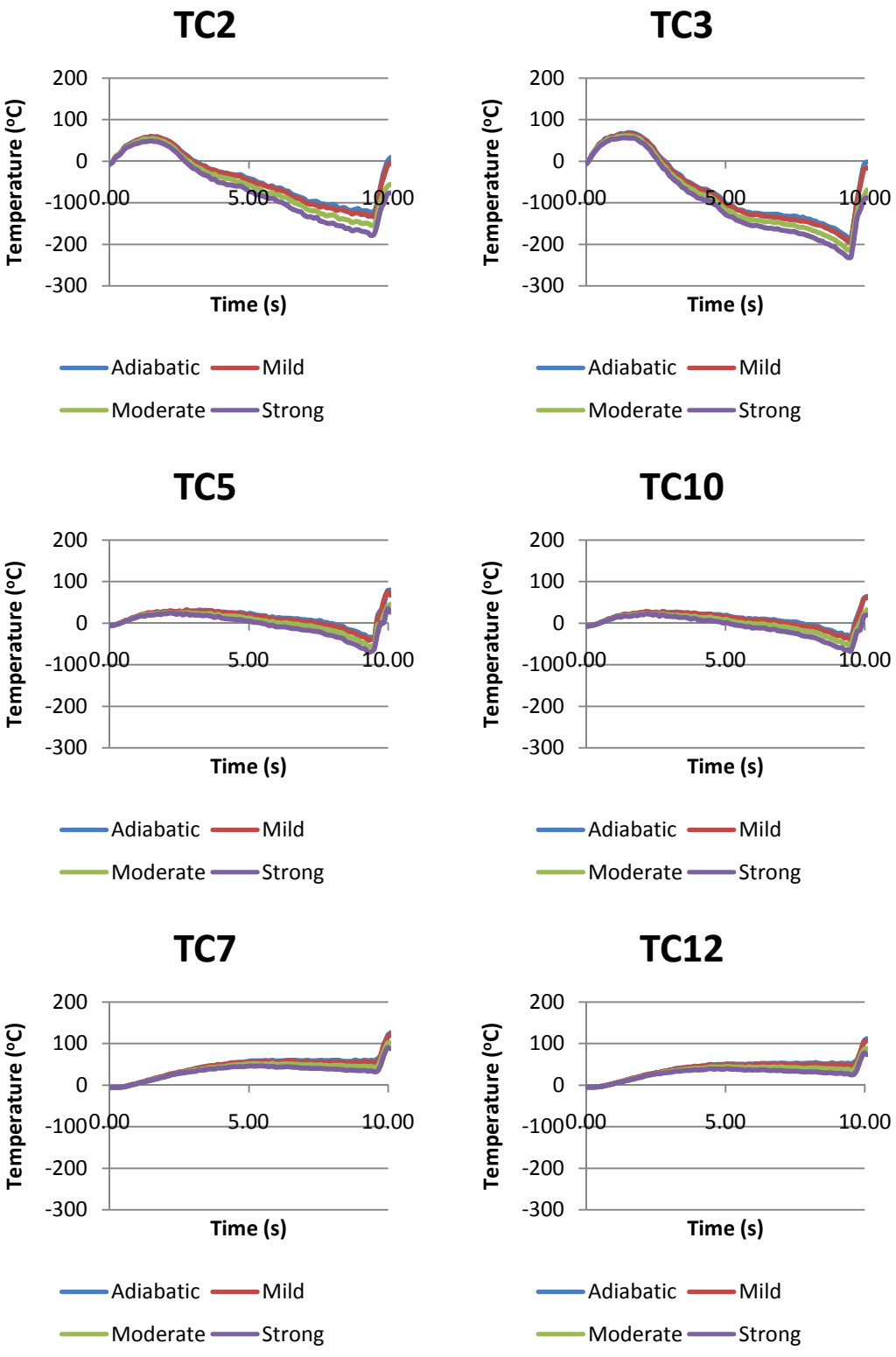

Figure 43 – Series of comparison plots showing different between experiment and heat transfer simulations.

4.3.4.Material Model Influence on Temperature Spread

4.3.4.1. Results

Temperature spread across the tested region is determined by looking at the difference of the temperature values at the inner-most and outer-most thermocouple locations. A study of the selected region allows an understanding of how quickly the heat generated at or near the tool-workpiece interface spreads itself through the medium. Figure 44 shows the closest and furthest thermocouple temperatures over the selected region plotted for the two depths of 3 and 6.5 mm. The two depths are used to focus on the temperature drop along a single depth within the tested region. It is significant to note the experimental temperature difference is significantly more than any simulation difference.

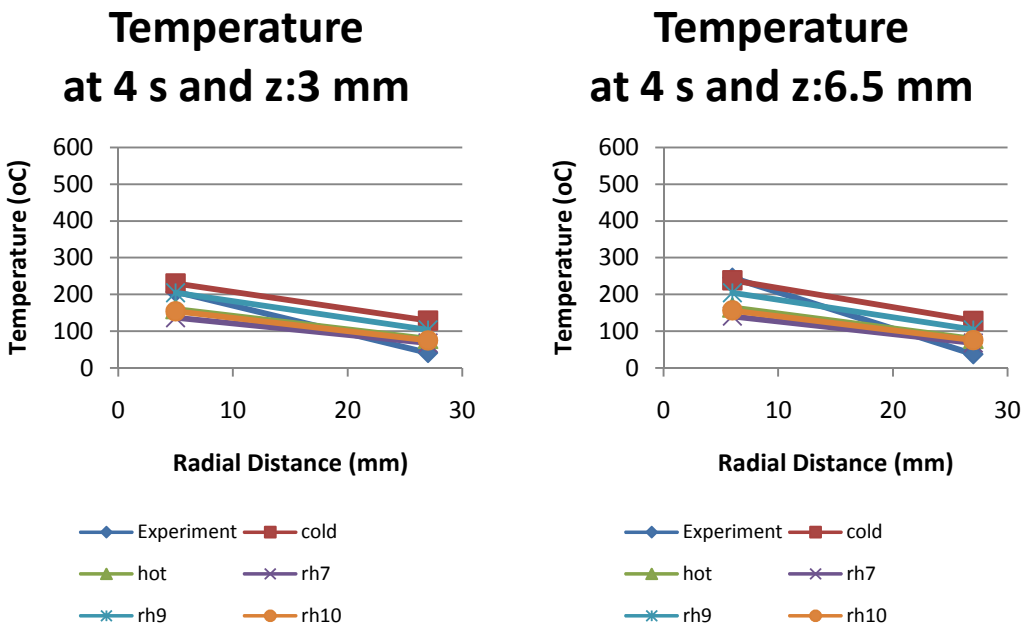

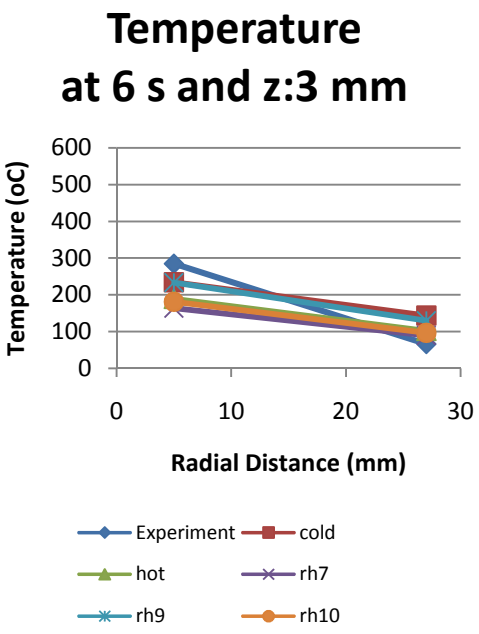
Temperature at 6 s and z:3 mm
Temperature (oC)
600
500
400
300
200
100
0
0
10
20
30
Radial Distance (mm)
Experiment
cold
hot
rh7
rh9
rh10

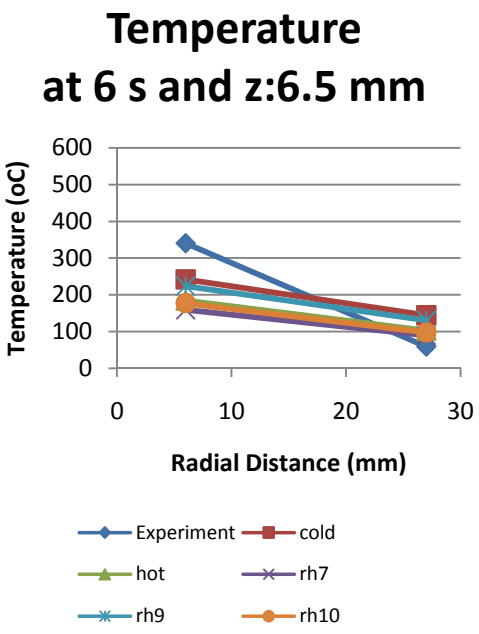
Temperature at 6 s and z:6.5 mm
Temperature (oC)
600
500
400
300
200
100
0
0
10
20
30
Radial Distance (mm)
Experiment
cold
hot
rh7
rh9
rh10

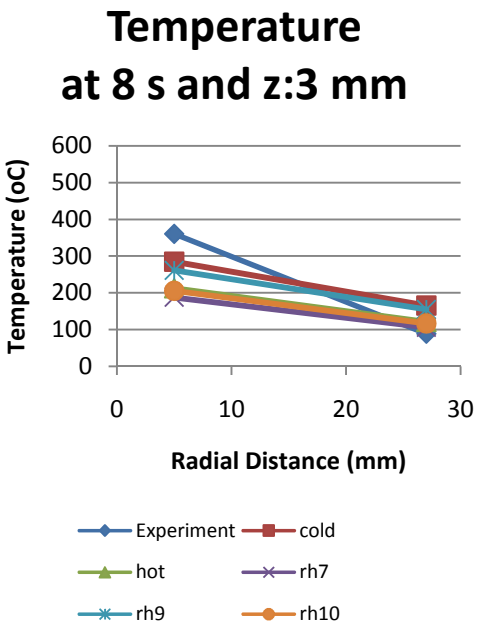
Temperature at 8 s and z:3 mm
Temperature (oC)
600
500
400
300
200
100
0
0
10
20
30
Radial Distance (mm)
Experiment
cold
hot
rh7
rh9
rh10

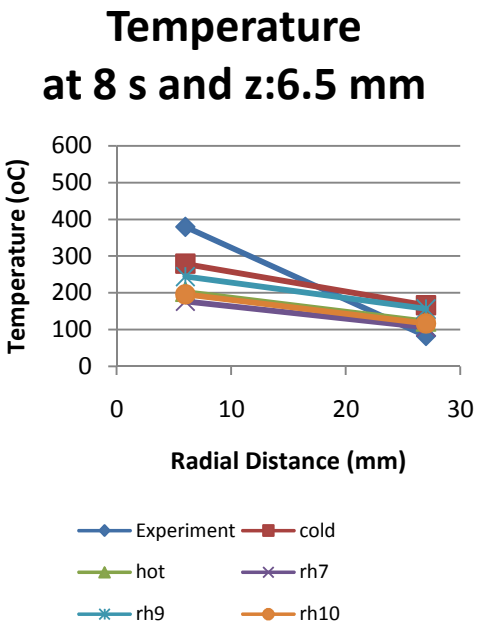
Temperature at 8 s and z:6.5 mm
Temperature (oC)
600
500
400
300
200
100
0
0
10
20
30
Radial Distance (mm)
Experiment
cold
hot
rh7
rh9
rh10

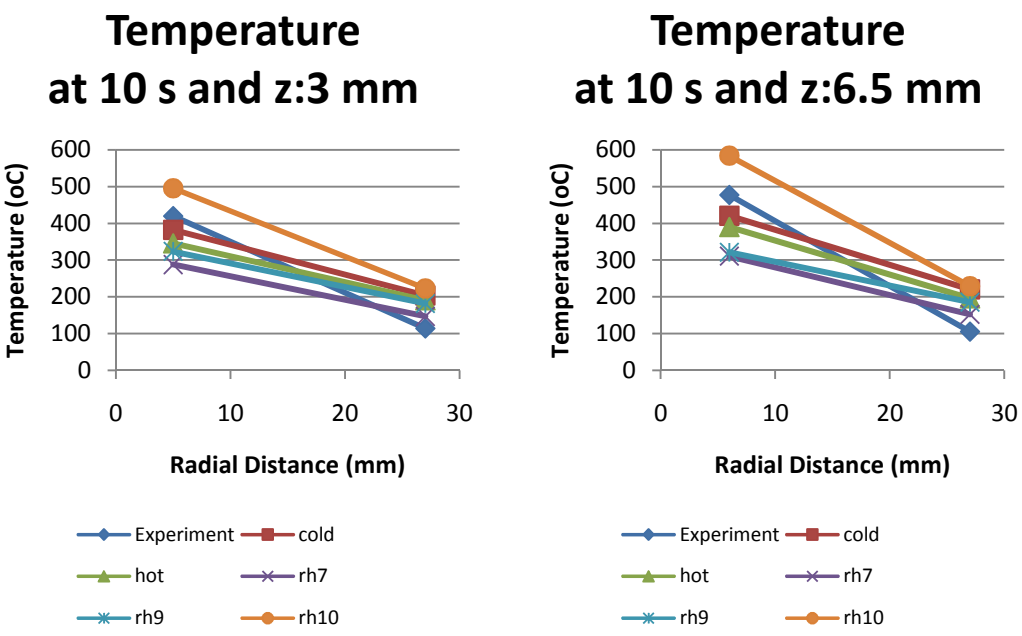

Figure 44 - Series of plot showing temperatures at the extremes of the sampled area at distinct times and depths.

4.3.4.2. Discussion of Results

The temperature difference between the inner and outer-most thermocouple is used to evaluate the different material models. To compare the experimental temperature difference to the experimental temperature differences a ratio of the differences is used. The temperature spread ratio is the ratio of the selected simulation temperature spread at a given time and location over the experimental temperature spread at the comparable point. A temperature spread ratio of 1 indicates that the spread of the simulation exactly matches the spread of the experiment. A ratio greater than 1 indicates the simulation has more spread than the experiment; a ratio less than 1 indicates the simulation has less spread. The plots of the temperature spread ratio are shown in Figure 45 and Figure 46.

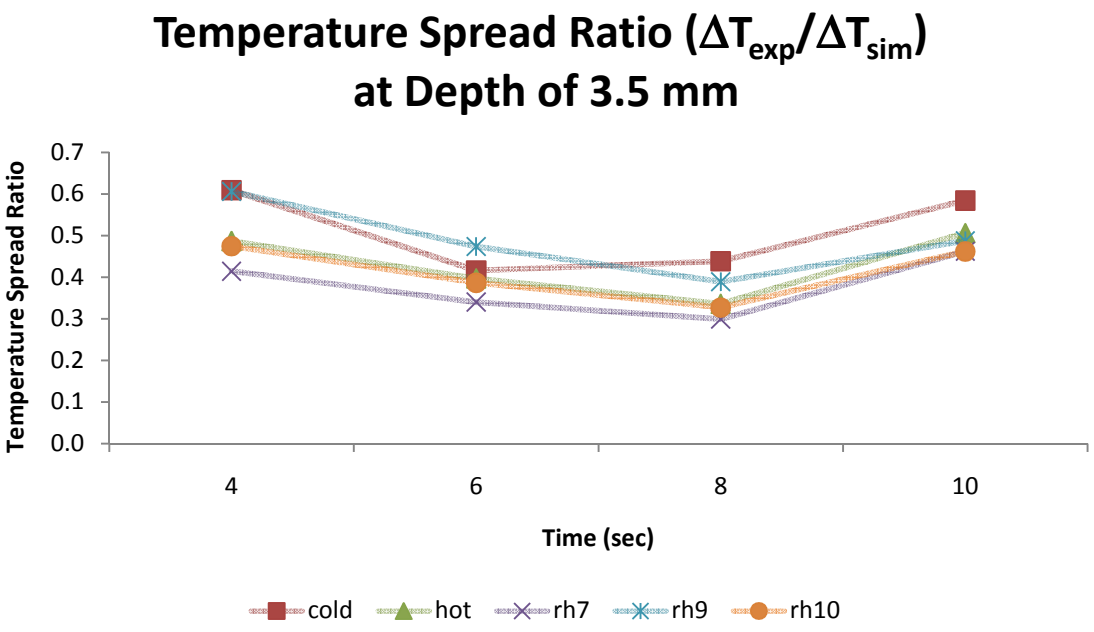

Figure 45 - Plot of temperature spread ratio over the tested interval at vertical depth of 3 mm.

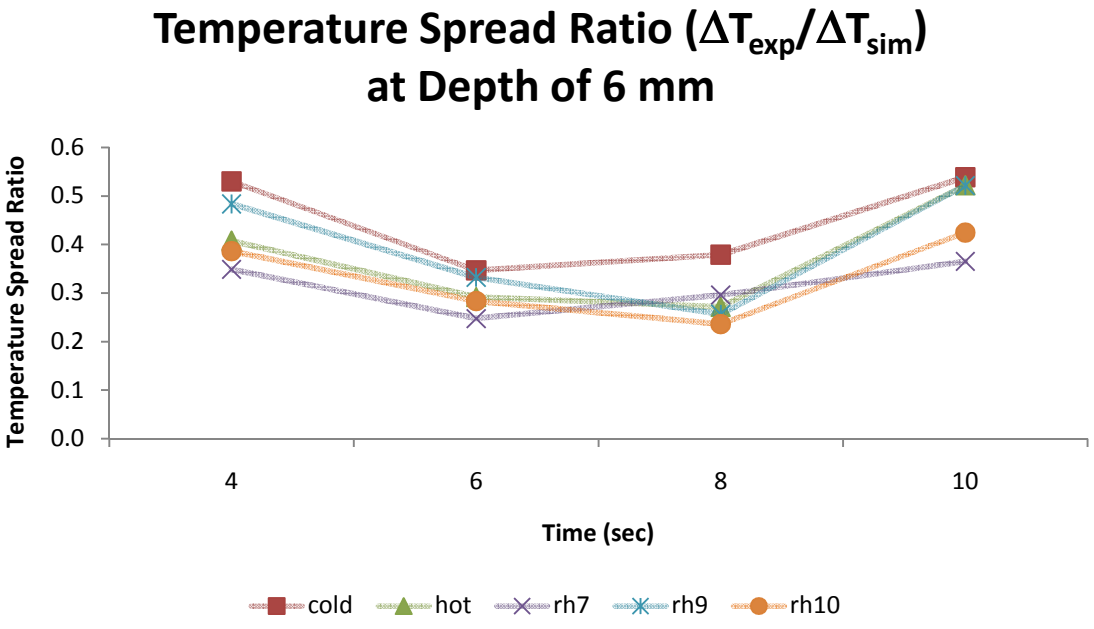

Figure 46 - Plot of temperature spread ratio over the tested interval at vertical depth of 6.5 mm.

A value of 0.5 in the plots above indicates the change between the inside thermocouple and outside thermocouple of the simulation is half that of the change for the experiment at that time and depth. The simulations of the plunge have a temperature spread between half and one third of the experimental temperature spread.

Each of the individual simulations has a distinct behavior that additionally characterizes its performance. The cold rheology simulation is generally the closest to the experiment across all of the simulation times, while the rh7 material model is generally the farthest. The hot material model is average in its performance at all times and depths. This result indicates that for the selected material models the hot material model has the least average discrepancy.

The simulations do not adequately model the temperature spread ratio at any of the simulated times. However at a time of 10 seconds, the error in temperature rise ratio is significantly reduced. This occurs as the simulations all experience a large temperature increase near the tool and the adjacent thermocouples react quickly to this change in peak temperature. The outside thermocouples in the simulation have not yet reacted to this change in peak temperature.

4.3.5.Material Model Influence on Average Temperature

4.3.5.1. Results

The different material models produce a variety of thermal behavior that can be compared to the measured temperatures to understand average temperature behavior. The average temperature across the thermocouples at a specified depth is calculated at 4 points in time during the plunge. Averages are calculated at two depths because the lower layers of thermocouples have a different range. Plots of these results are seen in Figure 47 and Figure 48.

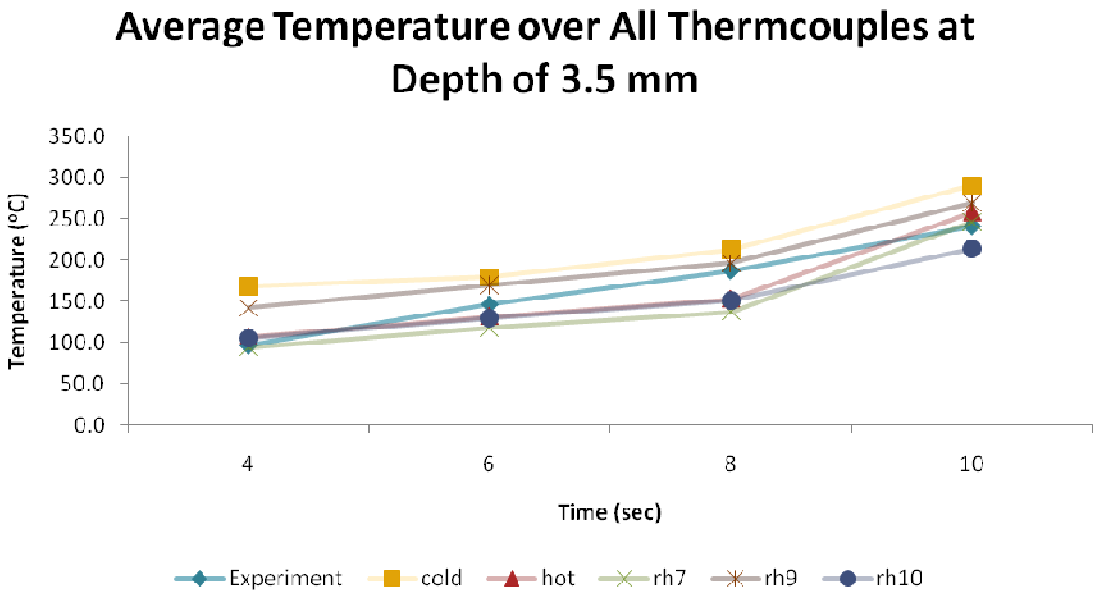

Figure 47 - Plot of average temperature across region of thermocouple distribution at distinct times for thermocouples located at a depth of 3.5 mm from the base.

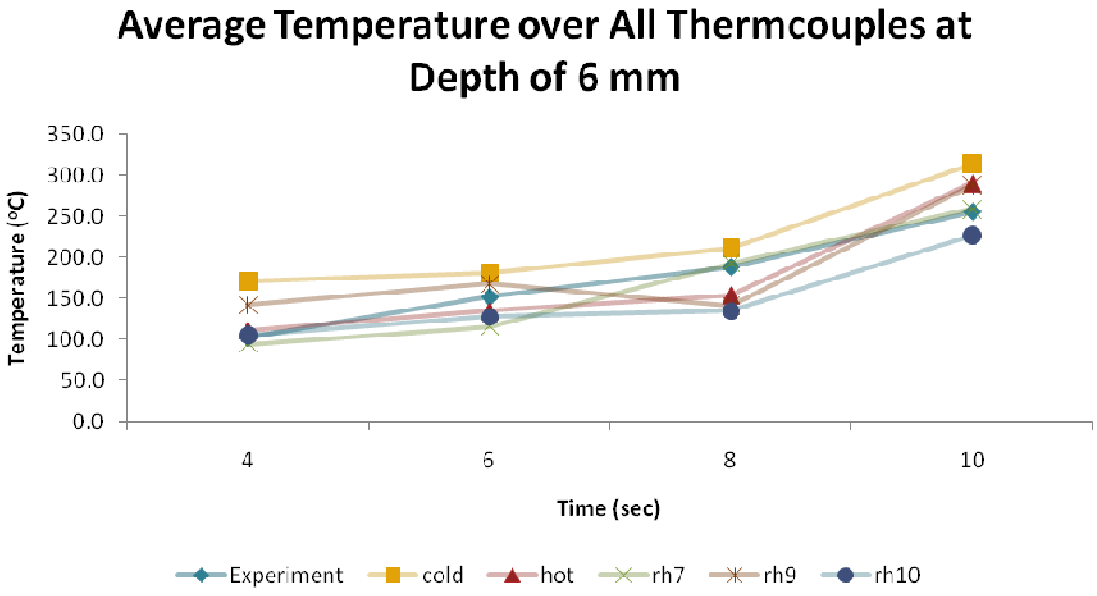

Figure 48 - Plot of average temperature across region of thermocouple distribution at distinct times for thermocouples located at a depth of 6mm from the base.

4.3.5.2. Discussion of Results

The experimentally measured temperatures are higher than some simulation temperatures and lower than other simulation temperatures. The cold material model serves as an upper bound for the average temperature while the rh10 material model generally serves as a lower bound of the selected simulations. Since the measured temperatures occur between these two material models, it is possible that a material model could be sufficiently adjusted to have a correct average temperature at each of these points in time.

Specific models show promise at matching the average temperature of the experiment. The rh7 model parallels the experimental measure at 8 and 10 seconds in the 6mm depth thermocouples. Most other material models show a sharp increase over that same interval that outpaces the rise of the simulation results. It is also notable that the rh9 material model has average results that are both above and below the material at specific points in time. The hot material model does not perfectly track the average temperature but is a reasonable approximation.

4.3.6.Summary of Model Improvements

The intent of this work was to improve the model of the friction stir process. The prior work used for comparison is that done by Oliphant (2004). His prior work and the current work is seen in Figure 49, Figure 50, Figure 51, and Figure 52.

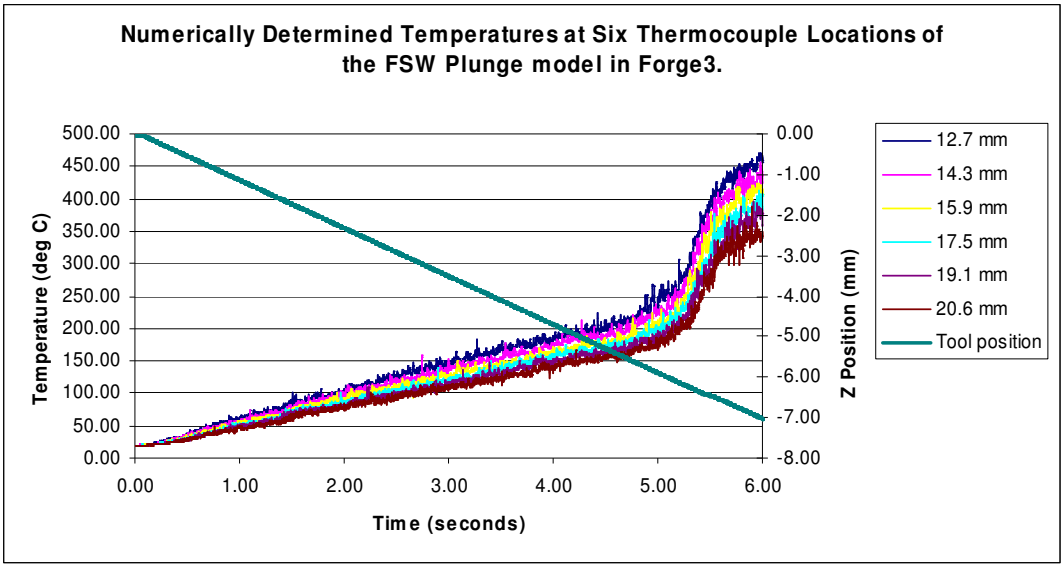

Figure 49 - Numerical simulation sensor data from Oliphant (2004) work.

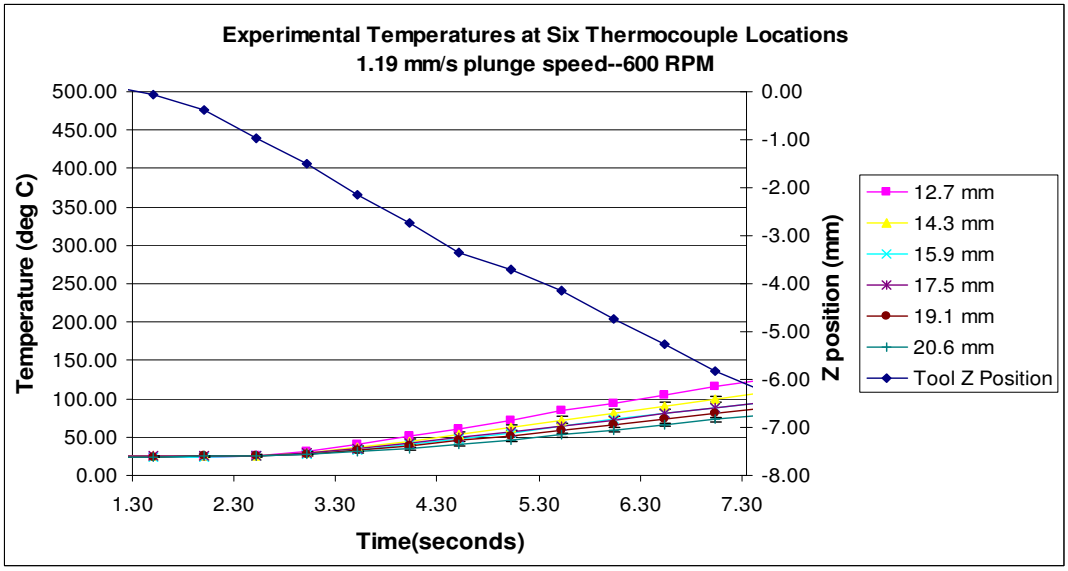

Figure 50 - Experimental thermocouple data from Oliphant (2004) work over 6 seconds.

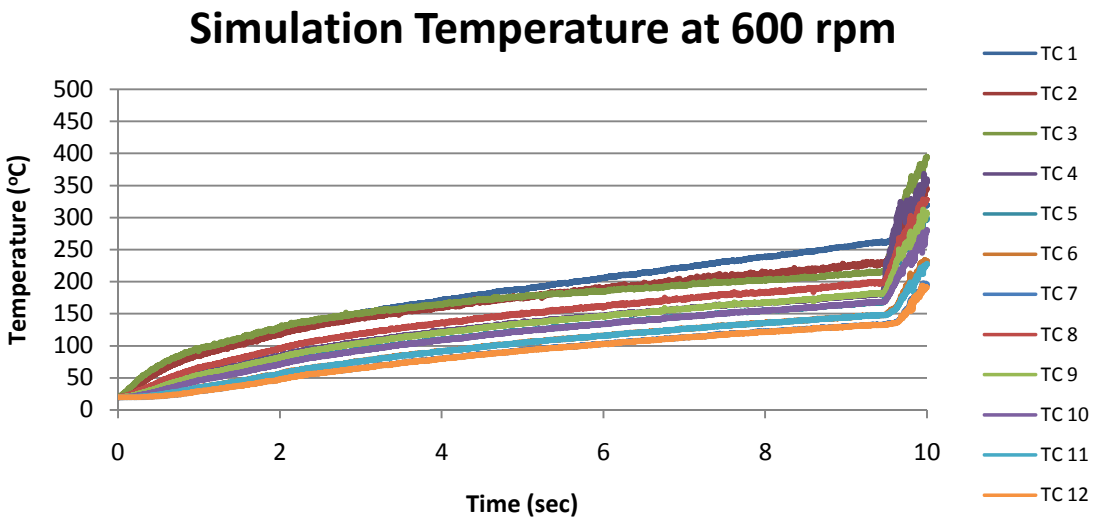

Figure 51- Numerical simulation sensor data from current work at strong heat transfer coefficient between the tool and workpiece, 600 rpm, medium mesh size, and hot material model.

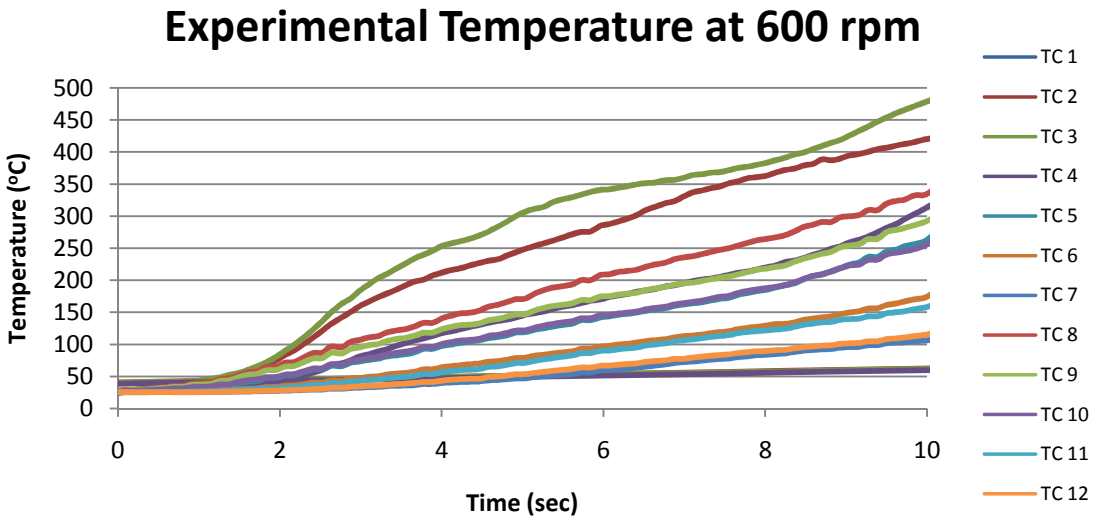

Figure 52– Experimental thermocouple data for 600 rpm spindle speed run.

Direct comparison is difficult as the time duration is different and the location of the thermocouples and sensors are different. TC4 can be used in comparison with the 12.4 mm radius location from Oliphant's work. A comparison at this location is seen in Figure 53. The Oliphant simulation over-predicts the experimental measures by over 300% at the best fit. The current simulation under predicts the experimental measures by less than 50% at the worst points.

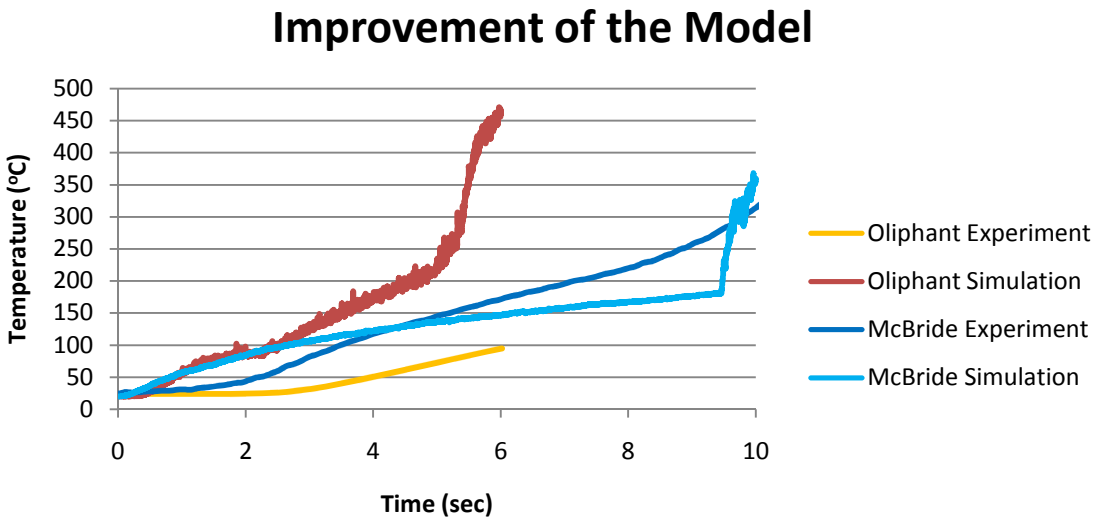

Figure 53 - Comparison of Oliphant (2004) experiment and simulation results and current experiment and simulation results.

5. Conclusions and Recommendations

5.1. Summary

Several parameters contribute to the composite behavior of the friction stir plunge. Within the plunge experimental, temperatures were compared with simulated temperatures to evaluate the quality of the prediction material. Forge2005 simulations are used to evaluate the influence of mesh size and the heat transfer coefficient on the numerical temperature result. Comparison of the experimental and simulations reveals the general behavior of the two methods, the significance of the heat transfer coefficient, and the influence of the material model.

5.1.1. Plunge Experiments

5.1.1.1. Spindle Speed Effect

There is a small but generally statistically significant increase in measured thermocouple temperature with increasing spindle speed. Using linear estimations for slope averaged from samples times at 4, 6, and 8 seconds for each of the thermocouple locations an average slope of .070^{o}C / rpm is representative of the behavior of the experiment. Relative to the large transient

changes that are occurring over the short plunge this small variation controlled by spindle speed is of minimal consequence to the friction stir plunge.

5.1.1.2. Dwell Results

Temperature stabilizes in the thermocouples closest to the tool (TC2, TC3, and TC4) during the dwell. Temperature continues to climb in the other measured areas during the dwell as heat continues to disperse through the medium.

5.1.2.Forge2005 Simulations

5.1.2.1. Mesh Size Influence

Mesh size significantly impacts the results of the simulation. However with the increased number of nodes the computation time dramatically increases. In selecting a balance between the duration and accuracy the medium mesh size of 3,000 nodes is sufficient.

5.1.2.2. Heat Transfer Coefficient Influence

The exchange of heat in the simulation, as regulated by the heat transfer coefficient, between the tool and the workpiece follows the convention that as the coefficient increases the temperature decreases by a proportion of .007%. A large increase in the heat transfer coefficient is required to make a change of more than a few ^{o}C in the workpiece.

5.1.3. Comparison

5.1.3.1. General Comparison of Temperature Curves

Model variations consistently show the simulation under-predicts temperature near the tool and over-predicts temperature far from the tool. While change in the material model does modify specific values of the resultant temperature the qualitative behavior is consistent in all observations. This indicates the simulations models require further refinement for before an exact model can be produced.

5.1.3.2. Comparative Spindle Speed Influence

Both the simulation and the experimentation show that with increased spindle speed the temperature in the workpiece increases. The spindle speed influence as a function of radius matches between the simulation and the experiment.

5.1.3.3. Heat Transfer Coefficient Significance

A wide range of heat transfer values was tested. Changes in the heat transfer coefficient had only a small effect on the simulation results relative to the changes that occur in the experimental temperatures over the course of a simulation.

5.1.3.4. Material Model Influence on Temperature Spread

Material model variations tested do not significantly impact the ability to model the temperature spread found in the area immediately around the tool. The results of these experiments show that the tested material models do not provide a good approximation of the temperature spread that occurs in the experimental temperatures. Other untested material models might provide a better match.

5.1.3.5. Material Model Influence on Average Temperature

Material model variations tested show that the average temperature across the interval can be modified by use of different material models. Some results of the selected simulation models show average temperatures below the experimental temperatures, while others show average temperatures above the experimental temperatures. This supports the possibility that the material model can be adjusted so that the mean temperature is in agreement with the experimental average temperature , but the specific material model that would lead to this result is not identified.

5.1.3.6. Summary of Model Improvements

Prior work done by Oliphant had the simulation over predicting the experimental measures by 300%. Current work reduces the over and under prediction to less than 50%. Efforts of this work have brought the experimental and simulation temperatures into closer agreement.

5.2. Future Work

Many opportunities exist for additional research in relation to the topics discussed in this work. A correct material model would allow researchers in all areas of numerical research to improve the model and better understand the parameter behaviors observed. This material model would require gleeble work and interpolative mapping for all necessary data points. Other thicknesses of material could be used to understand heat transfer and welding in the material. Thinner materials would allow the testing of weld strength. The users could also work to optimize additional parameters in the simulation. These parameters could include the use of EVP or Norton-Hoff based equations, the deformation increment, variable heat transfer coefficients and others. These additional parameters would allow for even more accuracy improvements in the model than were found in this work.

6. References

Thomas, W., Nicholas, E., Needham, J., Murch, M., Temple-Smith, P., Dawes, C., *Friction Stir Butt Welding*. International Patent Application No. PCT/GB92/02203. 1991.

Dong, P., Lu, F., Hong, J., Cao, Z., *Analysis of Weld Formation Process in Friction Stir Welding.* Proceedings of the 2nd International Symposium on Friction Stir Welding. Gothenburg Sweden. June 2000.

Song, M., Kovacevic, R. *Numerical and Experimental Study of the Heat Transfer Process in Friction Stir Welding.* Journal of Engineering Manufacture. Vol. 217. Part B. pp. 73-85. 2003.

Chen, C.M., Kovacevic, R. *Finite Element Modeling of Friction Stir Welding—Thermal and Thermomechanical Analysis.* International Journal of Machine Tools and Manufacture. Vol. 43. pp. 1319-1326. 2003.

Shi, Q., Dickerson, T., Shercliff, H. *Thermo-Mechanical FE Modeling of Friction Stir Welding of AL-2024 Including Tool Loads.* 4th International Symposium on Friction Stir Welding. Park City, UT. May 2003.

Chao, Y., Qi, X., Tang, W. *Heat Transfer in Friction Stir Welding—Experimental and Numerical Studies.* Journal of Manufacturing Science and Engineering. Vol. 125. pp. 138-145. 2003

Bendzsak, G., North, T., Smith, C., An *Experimentally Validated 3D Model for Friction Stir Welding*. Proceedings of the 2nd International Symposium on Friction Stir Welding. Gothenburg Sweden. June 2000.

Colegrove, P., Painter, M., Graham, D., Miller, T. *Three Dimensional Flow and Thermal Modelling of the Friction Stir Welding Process.* Proceedings of the 2nd International Symposium on Friction Stir Welding. Gothenburg Sweden. June 2000.

Ulysse, P. *Three-Dimensional Modeling of the Friction Stir Welding Process.* International Journal of Machine Tools and Manufacture. Vol. 42. pp. 1549-1557. 2002.

Oliphant, Alma. “Numerical Model of Friction Stir Welding: A Comparison of Alegra and Forge3”. Brigham Young University Library. 2004.

Lasley, Mark. “A Finite Element Simulation of Temperature and Material Flow in Friction Stir Welding”. Brigham Young University Library. 2005.

www.matweb.com. Internet. 15 June 2005.

Transvalor. *Forge2005 Users Guide.* Forge2005 Program Documentation. 2005.

Appendix A

Experimental Tool Design

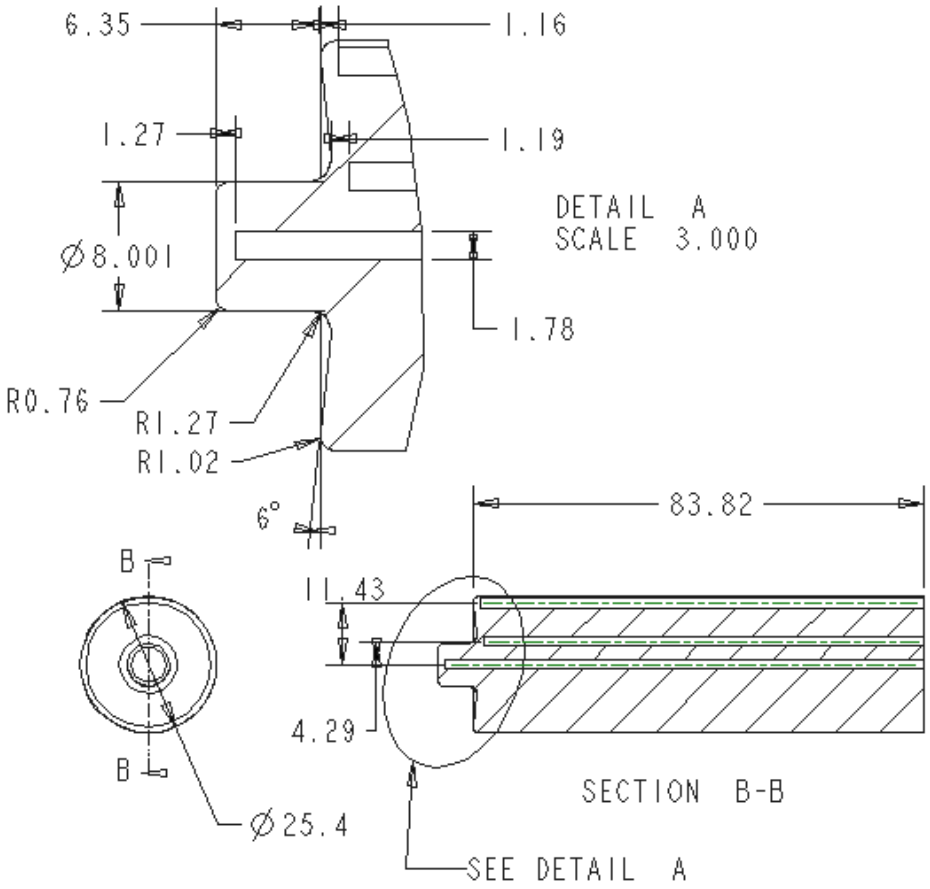

Figure 54 – CAD drawings of tool with holes for thermocouples.

Simulation Tool Geometry

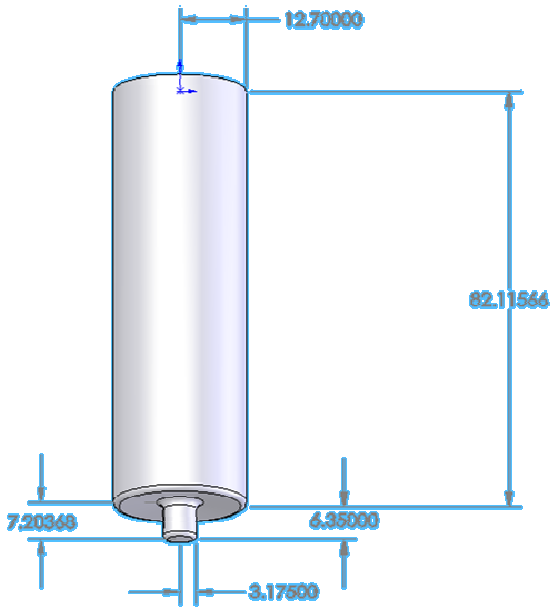

Figure 55 – CAD projection of tool geometry used in simulation.

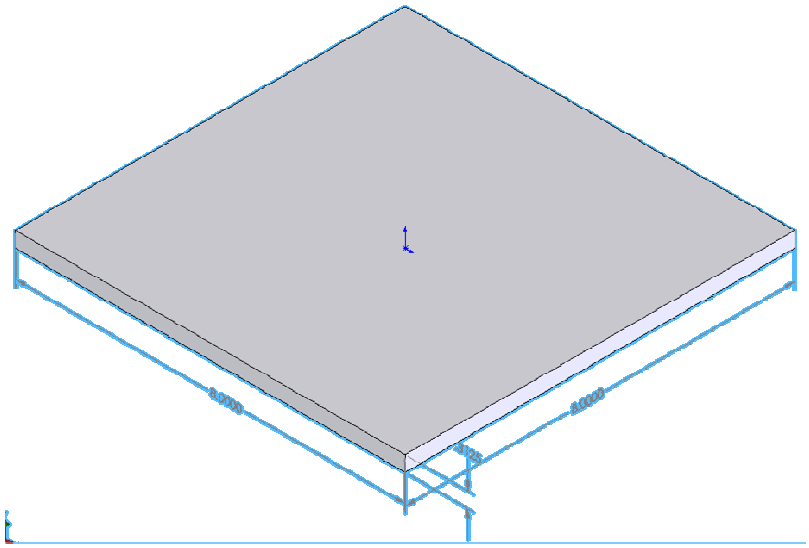

Figure 56 – CAD projection of workpiece geometry used in simulation.

Anvil System

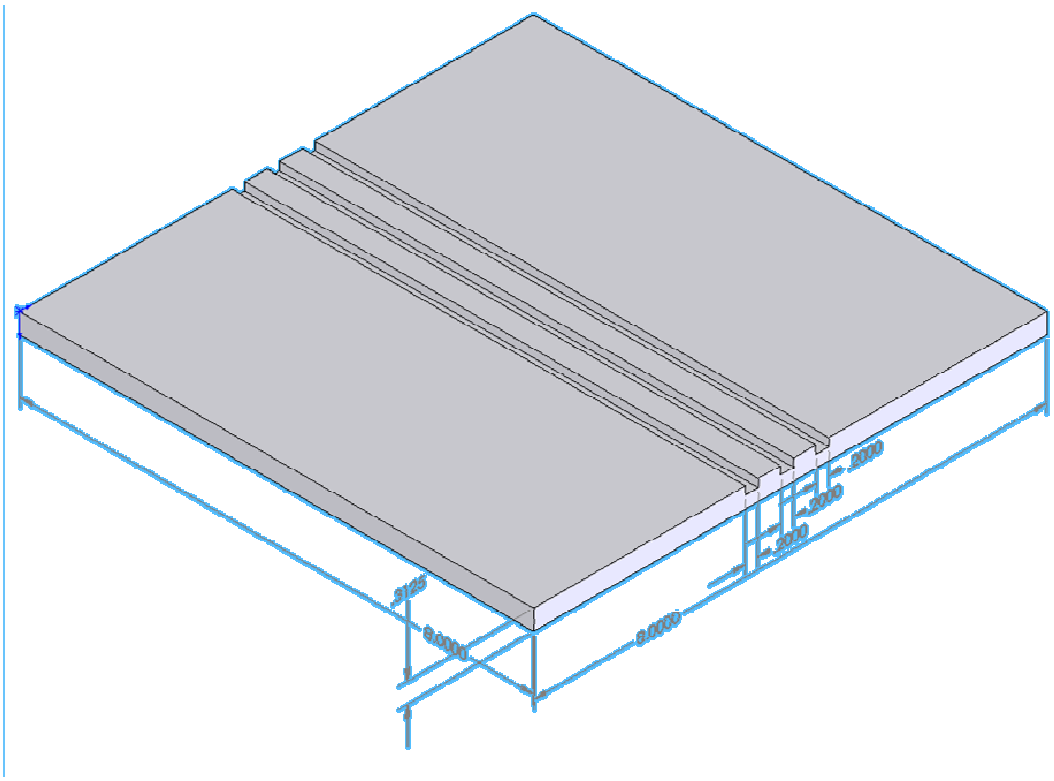

Figure 57 – CAD projection of secondary anvil allowing thermocouple probes to exit back of workpiece.

Test Specimens

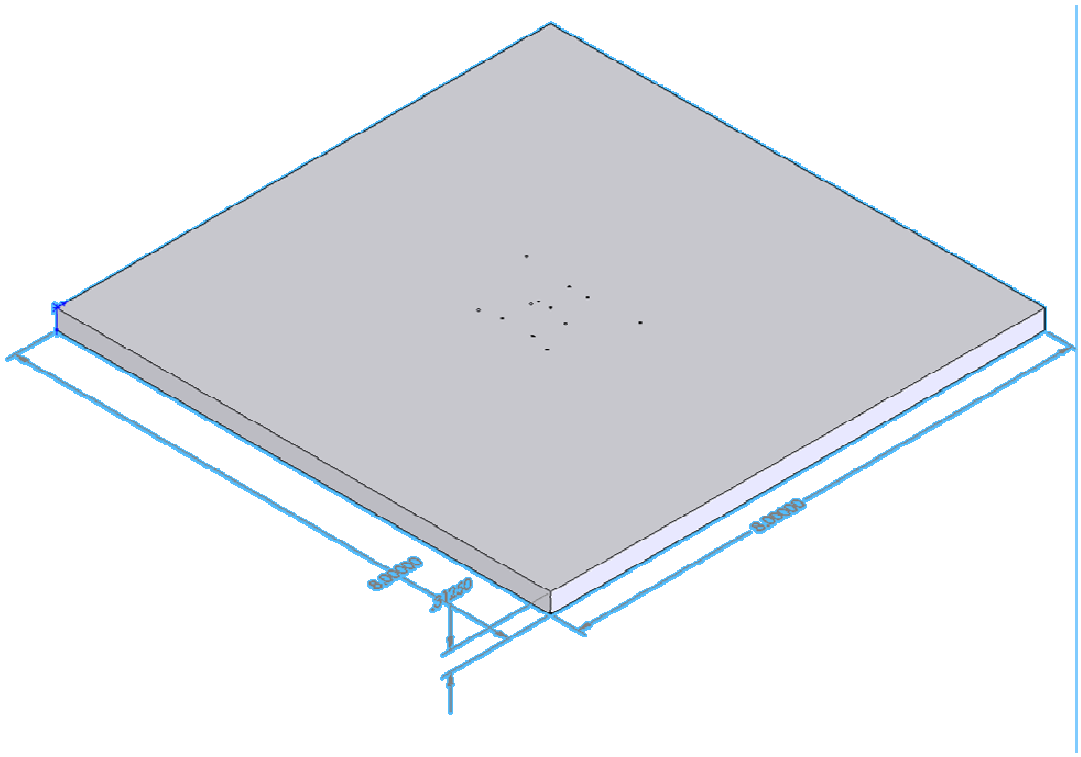

Figure 58 – CAD projection of test plate as seen from the back side.

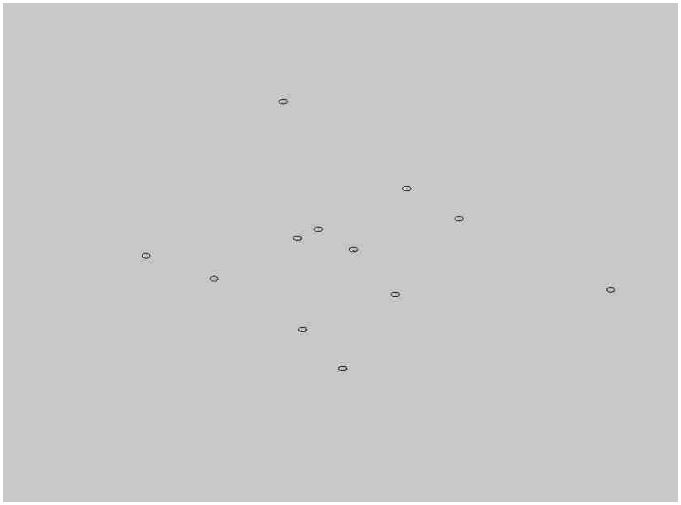

Figure 59 – Sketch of circular array of thermocouple holes found in back of test plate.